Thesis Approved

By

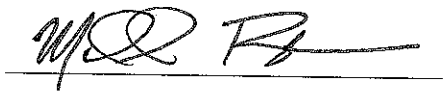

Major Advisor

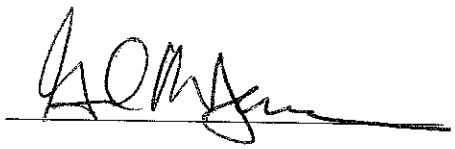

Dean

Committee Members:

Jason Bartz, PhD

Venkatesh Govindarajan, PhD

Nancy Hanson, PhD

Patrick Swanson, PhD

PURIFICATION OF HUMAN IMMUNODEFICENCY VIRUS TYPE 1 PREINTEGRATION COMPLEXES BY VELOCITY GRADIENT CENTRIFUGATION

By

Meghan Donnellan

A THESIS

Submitted to the faculty of the Graduate School of the Creighton University in Partial Fulfillment of the Requirements for the degree of Master of Science in the Department of Medical Microbiology and Immunology

Omaha, NE

December 11, 2009

Abstract

The early events of human immunodeficiency virus type 1 (HIV-1) infection are mediated by two large nucleoprotein complexes (NPCs), the reverse transcription complex (RTC) and the preintegration complex (PIC). These complexes are responsible for the conversion of viral RNA into viral DNA, transport through the cytoplasm, import into the nucleus, and the subsequent integration of the viral genomic DNA into the host chromosomal DNA. Several viral proteins are associated with the NPCs, including reverse transcriptase (RT), integrase (IN), viral protein R (Vpr), capsid (CA), matrix (MA), and nucleocapsid (NC). Previous studies of these complexes have yielded conflicting data, partially due to inconsistent production and purification methods. Here I examined several infection protocols and determined overnight (O/N) infection of C8166-45 cells via spinoculation to be the optimal production method to yield active PICs. I also evaluated the efficiency of several velocity gradient centrifugation (VGC) parameters for purifying NPCs. The sedimentation patterns of NPCs were determined by analyzing the distribution of known interacting viral proteins in gradient fractions. My results indicate that short velocity gradient centrifugation is preferred to extended centrifugation. Shorter centrifugation lengths separate the two NPCs instead of concentrating them as increased centrifugation does. Increased centrifugation also results in the dissociation of the complexes. These methods for the production and purification of HIV-1 nucleoprotein complexes will facilitate future proteomic analyses to identify novel HIV-1 cellular factors and hopefully lead to new targets for antiretroviral treatments.

Acknowledgments

There are so many people I would like to thank that have helped me along the way. This would not have been possible without help and guidance from Dr. Belshan. I would like to thank him for his patience (most of the time) as I was finding my way in research and especially during the writing process. It wasn't always easy, as we were both learning, but we made it through. I would also like to thank the members of my committee, Dr. Bartz, Dr. Hanson, Dr. Swanson, and Dr. Govindarajan, for their scientific guidance, suggestions, and discussions. My gratitude goes out to the members of Medical Microbiology and Immunology faculty and staff who supported me and advised me along my career path, especially Dr. Goering and Vonetta Byington. The decisions made were not easy and the advice and support was welcomed and I can't begin to express how thankful I am for that. I would also like to thank the friends I made in Graduate Student Government for keeping me sane and helping to balance my life while at Creighton. I appreciate all the prayers and moral support I have received over the years from the St. Luke's Episcopal Church in Chickasha, OK. Lastly, I would like to thank my parents, Jack and Gail Donnellan, my brother Ian Donnellan, and my extended family for being a constant support. I love you all and would not be the person I am today without you.

Table of Contents

List of Tables

List of figures

Abbreviations

CA	Capsid
DNA	Deoxyribonucleic Acid
DMEM	Dulbecco's Modified Eagle Medium
DPI	Days post infection
ERT-vDNA	Early reverse transcription product viral DNA
H.I.	Heat inactivated
HIV-1	Human Immunodeficiency Virus Type 1
hpi	Hours post infection
Hr	Hour
MA	Matrix
Min	Minute
Nev	Neveripine
O/N	Overnight
PCR	Polymerase Chain Reaction
PIC	Preintegration Complex
PVDF	Polyvinylidene flouride

Sec	Second
Spin.	Spinoculation
RNA	Ribonucleic Acid
RPMI	Royal Park Memorial Institute (medium)
RT	Reverse Transcriptase
RT-PCR	Reverse Transcription Polymerase Chain Reaction
RTC	Reverse Transcription Complex
TBS	Tris Buffered Saline
TBS-T	Tris Buffered Saline + Tween-20
vDNA	Viral DNA
VGC	Velocity gradient centrifugation
vRNA	Viral RNA
4 hpi- 5-45%/4 hr	4 hr gradients of 4 hr infected lysates
5-45%/1 hr	1 hr gradients of O/N infected lysates
5-45%/4 hr	4 hr gradients of O/N infected lysates

Introduction

Human immunodeficiency virus type 1 (HIV-1) is the etiological agent of acquired immune deficiency syndrome (AIDS). The World Health Organization estimates 33 million people were living with HIV in 2007 including 2.7 million newly infected persons world wide, and 2 million people died of HIV/AIDS the same year. Currently, there is no vaccine that prevents the spread of HIV-1. Once a person contracts HIV-1, there is no cure and the person must undergo treatment for the duration of their life. HIV-1 is a persistent infection, and many people may not know they are infected since early symptoms are generally mild and flu-like. Long term HIV-1 infection eventually leads to a decrease in CD4+ T cell counts and immune function. The resulting immune dysfunction leads to a variety of secondary, often opportunistic infections which eventually are fatal.

HIV-1 is a member of the lentivirus subfamily of the *retroviridae* family. The *retroviridae* are a family of single stranded RNA viruses that have two distinguishing characteristics. The first is an RNA-dependent DNA polymerase or reverse transcriptase enzyme which converts the single stranded viral genomic RNA into double stranded DNA. Second, the viral DNA (vDNA) is imported into the nucleus and integrated into the host chromosome. Lentiviruses are a unique subfamily of retroviruses in that they can infect non-dividing cells, such as macrophages.

The process of reverse transcription is highly error prone, resulting in a high mutation rate, which allows HIV-1 to rapidly evolve during infection. This high mutation rate results in a high rate of resistance when single drug therapy is used to treat patients; therefore, the use of multiple drugs is necessary for the long-term treatment of HIV-1 infected individuals. The predominantly used antiretroviral drugs target reverse

transcriptase and the protease enzyme necessary for virus maturation. There are also FDA approved inhibitors of the virus fusion protein and the integrase protein. Despite the use of multiple drug therapy, multidrug resistance has steadily risen over the last decade (Mocroft et al. 2004), even in individuals that have never been exposed to antiretrovirals (Perno et al. 2008). For this reason there is a continual need to develop new antiretroviral drugs. Potential targets for new inhibitors include viral assembly, uncoating, and nucleoprotein complexes (NPCs) that are critical for the early steps of HIV-1 replication.

Literature Review

Nucleoprotein complex composition: reverse transcription complex

The early events of HIV-1 infection are mediated by two large NPCs. These complexes are dedicated to synthesis of vDNA, its transport in to the nucleus, and its integration into chromosomal DNA. The first NPC, the reverse transcription complex (RTC), mediates the synthesis of double stranded vDNA from the single stranded viral RNA (vRNA). The RTC forms after uncoating of the incoming virion and consists of vRNA, reverse transcriptase (RT), nucleocapsid (NC), viral protein R (Vpr), and integrase (IN) (Greene and Peterlin 2002) as well as cellular proteins like HMGA1 (Greene and Peterlin 2002), BAF, LAP2α, and LEDGF/p75 (reviewed in Suzuki and Craigie 2007). When visualized by electron microscopy, the RTC is structurally observed to be a constant diameter cylinder of varying lengths during different stages of reverse transcription (McDonald et al. 2002).

Nucleoprotein complex composition: preintegration complex

Upon completion of reverse transcription the RTC is converted to the preintegration complex (PIC). The PIC mediates the integration of the vDNA into the host cell genomic DNA. It is operationally distinguished from the RTC *in vitro* by the ability to integrate vDNA into a heterologous DNA target. The complex undergoes several steps after reverse transcription is completed to form an active complex and integrate into the host chromosomal DNA (Greene and Peterlin 2002). First, integrase removes two nucleotides from the ends of the full-length vDNA by endonucleolytic

cleavage adjacent to a CA dinucleotide (Adamson and Freed 2008). This first reaction can occur in either the cytoplasm or the nucleus (Greene and Peterlin 2002). Next the vDNA inserts into the host chromosomal DNA via a strand transfer reaction (Adamson and Freed 2008). Strand transfer is initiated by cleavage of the host DNA (4 – 6 base pairs), followed by a transesterification reaction that joins the cleaved host and viral DNA. The reaction results in gaps in the DNA which are repaired by cellular DNA repair machinery possibly in conjunction with IN (Adamson and Freed 2008).

Purification of nucleoprotein complexes

As mentioned, the RTC and PIC represent potential targets for antiretroviral drug development. Both the RTC and PIC have been extensively studied, but more information about the early NPCs' composition, assembly, and transport is needed before targeted research into inhibitor development is warranted. Many questions remain, including how the complexes assemble, whether the complexes are discrete from each other, what their cellular composition is, and how the complexes transport into the nucleus of cells. Composition studies of the RTC and PIC have produced inconsistent data. One possible reason for the inconsistencies is that several different methods have been used to purify HIV-1 NPCs. These include size exclusion chromatography (Bukrinsky et al. 1993; Miller, Farnet, and Bushman 1997; Farnet and Haseltine 1991), and both density and velocity gradients (Miller, Farnet, and Bushman 1997; Farnet and Haseltine 1991; Bukrinsky et al. 1993; Farnet and Haseltine 1990; Fassati and Goff 2001). Each of these methods has limitations for the purification of large NPCs. For example, the HIV-1 NPCs typically elute in the void/excluded volume when purified by size exclusion chromatography (Bukrinsky et al. 1993; Miller, Farnet,

and Bushman 1997; Farnet and Haseltine 1991) unless DMSO is added (Miller, Farnet, and Bushman 1997). Gradients, which can purify molecules by size or density historically suffer from inconsistent formation and diffuse fractionation and may result in disintegration of the complexes under centrifugal stress.

Although the only protein required for vDNA integration *in vitro* is integrase (Farnet and Haseltine 1990), studies have detected other viral components to be associated with the PIC and/or required for efficient completion of the early steps of HIV-1 replication. The association of matrix (MA) with NPCs is controversial. An early report by Bukrinsky et al. (1993) observed MA to associate with NPCs when the cells were lysed with hypotonic buffer; however MA dissociated from NPCs when cells were lysed with mild detergent. Contrasting that report Miller, Farnet, and Bushman (1997) detected MA in NPCs from cells lysed with a mild detergent and Fassati and Goff (2001) could not detect any MA associated with NPCs from cells lysed with hypotonic buffer. Capsid (CA) was observed to dissociate from the RTC in HIV-1 infected cells (Bukrinsky et al. 1993; Farnet and Haseltine 1990; Fassati and Goff 2001), yet recent studies have suggested that a proper rate of CA uncoating is critical for nuclear import of the PIC in non-dividing cells (Dismuke and Aiken 2006). Vpr is associated with the PIC (Fassati and Goff 2001) and seems to be necessary for efficient nuclear transport of the PIC in non-dividing cells (Heinzinger et al. 1994). RT activity has also been observed in purified PICs (Miller, Farnet, and Bushman 1997; Fassati and Goff 2001) although no functional significance has been defined. NC binds to vDNA (Lapadat-Tapolsky et al. 1993) and is necessary for efficient nuclear import (Mougel, Houzet, and Darlix 2009; Poljak et al. 2003), however has not been biochemically shown to associate with the PIC.

Nucleoprotein complex cellular transport

Recent studies have begun to uncover how the RTC/PIC transport through the cell. Both actin and microtubules seem to be involved in the HIV-1 NPC transport since the disruption of both cytoskeletal elements is necessary to ablate NPC movement through the cytoplasm (McDonald et al. 2002). Live cell imaging indicates the early molecular motion of the RTC in the cytoplasm is characteristic of microtubule movement. Closer to the nucleus the movement of the complexes slows to a speed characteristic of actin mediated transport (Arhel et al. 2007). How the complexes associate with these cytoskeletal elements or what mediates the transition between them has not been biochemically determined.

Nucleoprotein complex nuclear import

The mechanism of PIC entry into the nucleus also remains unresolved. The estimated size of the PIC (160 – 320 S value; Bowerman et al. 1989; Karageorgos, Li, and Burrell 1993) suggests a complex structure incapable of passively entering the nucleus. Moreover, nuclear entry of the PIC is an energy dependent process (Moore and Blobel 1992; Bukrinsky et al. 1992). Several viral proteins have been shown to participate in nuclear import of the PIC, including MA (Gallay et al. 1995; Gallay et al. 1996), IN (Yamashita and Emerman 2005; Armon-Omer, Graessmann, and Loyter 2004), and Vpr (Heinzinger et al. 1994; Gallay et al. 1996). However, none of these proteins or their nuclear localization signals has been shown to be critical for PIC nuclear import. Recent reports have also suggested that CA regulates the nucleophilic properties of PICs. Mutations in CA that delay its uncoating from the NPC results in a reduction in PIC import into the nucleus (Yamashita et al. 2007). Several cellular

proteins have also been implicated in nuclear import including Imp7 (Fassati et al. 2003), transportin-SR2 (TRN-SR2; Christ et al. 2008), nucleoporin 98 (Nup98; Ebina et al. 2004), and Nup153 (Woodward et al. 2009). These proteins suggest that the use of nuclear import pathways are complex, involving the use of multiple or redundant pathways.

Due to their labile nature and low concentrations in infected cells the NPCs present during the early steps of HIV-1 infection are difficult to study. The purification methods used to extract the NPCs likely alter the structure and composition of the recovered complexes. A method to efficiently produce and purify RTCs and PICs is the first critical step toward additional biochemical and proteomic studies that will further our understanding of the architecture and transport of both complexes. In these studies we set out to develop methodologies to purify RTCs and PICs for biochemical and proteomic studies. Using velocity gradient centrifugation (VGC) we were able to partially purify RTCs and active PICs. The presence of RTCs was confirmed by the co-sedimentation of vRNA, RT activity, and ERT-vDNA. PICs were identified in fractions by the presence of vDNA and *in vitro* integration activity. After testing several infection protocols and gradient centrifugation lengths we defined a protocol capable of separating the components of RTCs from PICs. These studies are the necessary first step toward identifying new potential targets for antiretroviral drug development.

Materials and Methods

Tissue culture

293TK cells (a kind gift from Tom Hope) were grown in 10 cm dishes in complete Dulbecco's Modified Eagle Medium (DMEM; Invitrogen, Carlsbad, CA) supplemented with 10% fetalclone III (Hyclone, Logan, UT), 100 U/ml penicillin, 100 μg/ml streptomycin and L-glutamine (final concentration 592 mg/L; Invitrogen). 293T.BirA cells (Belshan et al. 2009) were grown in 10 cm dishes in complete DMEM with 10 μg/ml Blasticidin S (InvivoGen, San Diego, CA). C8166-45 (Engleman, 2009) and SupT1 cells (Smith et al. 1984) were cultured in complete Royal Park Memorial Institute medium (RPMI; Invitorgen) supplemented with 10% fetalclone III, 100 U/ml penicillin, 100 μg/ml streptomycin and L-glutamine. All cells were cultured in humidified incubators with 5% CO_2 at 37°C. At least every two months incubators were cleaned with TB-Cide Quat (Spartan Chemical Company, Maumee, OH), 70% ethanol, and the internal components sterilized by autoclaving.

Production of HIV-1 stocks

Pseudotyped virus was produced by transient transfection of 293TK cells using TransIT-LT1 reagent, based upon manufacturer's recommendations (Mirus, Madison, WI). 293TK cells were seeded in 10 cm plates at a confluency of 30 – 40% (~$2x10^6$ cells) one day before transfection. Prior to transfection, a transfection mixture was made by first combining 12 μg pNLX HIV-1 molecular clone (a kind gift from Alan Engelman; Brown et al. 1999) and 5 μg pMD2.G vesicular stomatitis virus glycoprotein (VSVg) expression vector (Addgene, Cambridge, MA) in a 0.6 ml tube. Separately, 52 μl of

Transit-LT1 was added to 1 ml of Opti-MEM (Invitrogen), vortexed, centrifuged briefly, and incubated at room temperature for 5 min. The molecular clone and envelope expression vector mixture was then added to Opti-MEM, inverted to mix, briefly centrifuged, and incubated at room temperature for 5 min. The media on the 293TK cells was replaced with fresh, complete DMEM lacking phenol red (Invitrogen). The plasmid-TransIT-LT1 mixture was added, drop-wise, to the culture plates ensuring complete coverage of cells, and the plates were returned to the incubator. Media was collected every 24 hr for 3 days and stored at 4°C. After the last collection, the cellular debris was removed by centrifugation for 5 min at 250 x*g*. Virus supernatant was concentrated by column filtration using 100,000 MWCO filters as directed by the manufacturer (Millipore, Billerica, MA). Briefly, 15 ml of supernatant was added to the column and centrifuged at 4,000 x*g* at 4°C for 20 min. The flow-through was discarded and the process repeated until all the virus supernatant was added to the column. The concentrated virus sample was transferred to a new vial and the residual virus recovered from the filter by rinsing with Opti-MEM. If necessary, Opti-MEM was added to bring the total concentrated virus volume up to an equivalent of 4 ml per 10 cm dish. Concentrated virus was divided into 1 ml aliquots and stored at -80°C.

Production of preintegration complexes (PICs)

PIC production is based upon previously described methods (Belshan et al. 2009; Engelman 2009). Virus stocks were thawed and treated with 50 μl Turbo DNase and 117 μl 10X buffer (Ambion, Austin, TX) for 60 min at 37°C prior to infecting cells. A culture of 100 ml of C8166-45 cells was grown to approximately $1x10^6$ cells/ml for each infection ($1x10^8$ total cells). Cells were pelleted by centrifugation for 4 min at 250 x*g* and

resuspended with the DNase-treated virus. Each virus-cell mixture was transferred to a well of a six well plate containing 1 ml of complete RPMI and 32 μg/ml polybrene (final concentration 16 μg/ml). The plate was incubated for 10 min at room temperature to allow the cells to settle to the bottom of each well. This was important to maintain an even layer of cells during spinoculation. Cells were spinoculated (O'Doherty et al. 2000) by centrifugation at 1050 x*g* for 2 hr at 25°C using a biosafety rotor. At the end of spinoculation the plates were cultured at 37°C for 1 hr. The volume of complete RPMI added to the cell cultures depended on the infection length: for 4 or 6 hr infections, 2 ml of media were added to each well; and for overnight (O/N) infections, cell media was brought up to a volume of 42 ml (2 ml of cell culture, 5 ml of media used to wash the wells, and 35 ml of media) in a 75 cm^2 tissue culture flask.

After infection, the cells were transferred to either 15 ml (4 hr or 6 hr infections) or 50 ml (O/N infections) conical vials and pelleted at 250 x*g* for 4 min at 4°C. The media was discarded and the cells washed (resuspended and pelleted) twice with 5 ml Buffer K(-) (20 mM HEPES (pH 7.5), 150 mM KCl, 5 mM $MgCl_2$). After the second wash the cells were lysed with 1.5 ml of Buffer K+/+ (Buffer K(-) supplemented with 0.1% DTT and 1X Protease Inhibitor Cocktail IV (EMB Biosciences, Gibbstown, NJ)) and 0.1% TritonX-100 in 2 ml tubes by gentle rotation for 40 min at 4°C. The nuclei were removed by centrifugation (1000 x*g* for 5 min), the supernatant transferred to a 1.6 ml tube, and the lysates further clarified by centrifugation at 21,000 x*g* for 5 min. If replicate infections were performed, the supernatants were combined at this point. 100 μl was removed for viral DNA (vDNA) isolation as described below. Lysates were then separated into 550 μl aliquots, flash frozen by immersion in liquid nitrogen, and stored at -80°C.

Production of gradients

Gradients were made in 14 × 89 mm open-top polyclear centrifuge tubes (Seton Scientific, Las Gatos, CA) which were pre-rinsed three times with millipure water and dried. Gradients were formed utilizing the Gradient Master Station as described by, and using parameters provided by the manufacturer (BioComp, Fredericton, NB, Canada). Briefly, 5% sucrose ((w/v) in Buffer K) was added using a syringe with attached cannula to the bottom half of the tube as measured with the manufacturer's short cap Marker Block (~ 6.5 ml). The tube was filled using a second cannula to slowly add 45% sucrose ((w/v) in Buffer K) to the bottom of the tube. The tubes were sealed with the provided short caps, and the excess sucrose solution removed from the top of the cap. Prior to running the gradient protocol, the plate on the Gradient Station was leveled and the centrifuge tube holder placed in the center of the plate. The gradients were formed by executing the manufacturer's specific protocol for 5-45% sucrose gradients (1 min 24 sec rotation at an 81.5° angle and speed of 21 rpm). After formation, the gradients were kept on ice until used. The gradient caps were removed and 500 μl discarded from the top of the gradient to accommodate samples. 500 μl of lysate was layered drop-wise on top of each gradient. The tubes were wiped to remove residual moisture, placed in the SW41 swinging bucket, and sealed. Ultracentrifugation was performed with an LE-80 Ultracentrifuge (Beckman Coulter, Fullerton, CA). The parameters vary by experiment, but all used slow acceleration and slow deceleration.

Fractionation of gradients

The fractions were collected using the piston fractionator on the Gradient Master Station. Prior to fractionation the reservoir was filled and the fractionator washed twice

with cold Buffer K(-). The piston was lowered slowly into the tube until sample was seen in the sample collection line (~ 1 inch). Fractions were collected at the speed of 0.5, distance 0.395, for a total distance of 82.95 or 21 fractions. The fractions were collected in 15 ml conical tubes or 1.6 ml tubes for concentration or single gradients, respectively. Tubes were kept on ice during fractionation and inverted several times to mix before any samples were removed. The linearity of gradients was monitored by measuring the refractive index of a 15 µl sample of each fraction using a refractometer (Thermo Scientific, Pittsburgh, PA). Gradient fractions were stored at 4˚C until use.

Concentration of gradient fractions

Gradient fractions were concentrated using 3,000 MWCO column concentrating filters as directed by the manufacturer (Millipore). The same volume (3 ml) of each gradient fraction and 0.5 ml of Buffer K(-) was added to concentrating columns. The columns were centrifuged for 20 min at 4,000 x*g* at 4°C. After centrifugation the flow through was discarded, the column refilled with Buffer K(-), and the sample re-centrifuged. This process was repeated twice for fractions 1 – 9 and three times for fractions 10 – pellet. The fractions were concentrated to a volume less than or equal to 500 µl as determined by the markings on the filter concentrator. The concentrated sample was transferred to a 1.6 ml tube and the residual protein was recovered by rinsing the filter with 100 µl Buffer K(-). The amount of sample was measured with a 1000 µl pipette and each sample brought up to a volume of 650 µl with Buffer K(-). The refractive index of each sample was measured to the ensure concentration was below 5% (w/v) sucrose. If not, the samples were returned to the column, more Buffer K(-) added, and re-centrifuged until the refractive index indicated less than 5% (w/v) sucrose.

Extraction of viral DNA from lysates and gradient fractions

DNA was isolated from samples (lysates or gradient fractions) using PureLink PCR Purification Kit (Invitrogen) with a vacuum manifold (Qiagen, Valencia, CA) according to manufacturers protocol. Briefly, 400 μl of Binding Buffer (4:1 ratio) was mixed with 100 μl of each sample by inversion, transferred to the anion-exchange column and the vacuum applied. Columns were washed with 650 μl Wash Buffer. Columns were then removed from vacuum and centrifuged at 21,000 x*g* for 2 min to remove residual buffer. To recover vDNA, columns were placed in a 1.6 ml elution tube, 50 μl of Tris-EDTA (pre-warmed to 65°C) added to each column, incubated at room temperature for 1 min, and centrifuged for 1 min at 21,000 x*g*. vDNA samples were stored at -20°C.

Detection of vDNA by quantitative real-time PCR

The sequences of all primers used for PCR and RT-PCR are listed in Table 1. The standards used for quantitative detection of vDNA and vRNA by real-time PCR were a dilution series of the pNLX plasmid (Brown, Chen, and Engelman 1999). Standards were made in 3 ng/μl tRNA at concentrations of 100,000, 10,000, 1,000, 100, and 10 fg/μl. PCR reactions were set up on ice in a PCR cabinet (Streamline Laboratory Products, Fort Myers, FL). Each 20 μl reaction contained: 7.8 μl distilled water, 10 μl 2X IQ SybrGreen Supermix (Bio-Rad, Hercules, CA), 250nm NL919 primer, 250 nM cNL1054 primers, and 2 μl of standard or vDNA sample. Reactions were performed in a 96-well PCR plate covered with optically clear flat top caps. The plate was cut into sections and the samples briefly centrifuged to remove any air bubbles. Real-time PCR was performed using an iQ5 Multicolor real-time PCR detection system (Bio-Rad). The

Application	Target	Name	Sequence
vDNA; vRNA	*gag*-specific	NL919 cNL1054	ttc gca gtt aat cct ggc ctt gca cac aat aga gga ctg cta ttg ta
ERT-vDNA	ERT product	NL497 cNL574	gct aac tag gga acc cac tgc tt aca aca gac ggg cac aca cta c
Integration assay (first PCR)	Plasmid target Internal HIV-1	pTZ19R2413 pTZ19R2414 L-cNL653	gtt gtt cca gtt tgg aac aag agt c act caa ccc tat ctc ggt cta ttc atg cca cgt aag cga aac tgc gtc cct gtt cgg gcg cc
Integration assay (real-time PCR)	Linker Internal HIV-1	L-primer NL506	atg cca cgt aag cga aac tgc gaa ccc act gct taa gcc tc
pTZ19R-LTR standard construction	LTR vDNA insert HIV-1 vector Sequencing	NL1-BH1 cNL702Pst1 NL1 cNL702 T7 primer	gcg gga tcc tgg aag ggc taa ttt ggt cc gcg ctg cag gcc gag tcc tgc gtc gag ag tgg aag ggc taa ttt ggt cc gcc gag tcc tgc gtc gag ag ata cga ctc act ata gg

PCR parameters were: an initial denaturing step at 95°C for 6 min; followed by 38 cycles of: 1) denaturing at 95°C for 20 sec, 2) annealing at 55°C for 20 sec, and 3) extension at 72°C for 30 sec. The real-time capture occurred during the extension step.

Extraction of viral RNA from Gradient Fractions

RNA was extracted from gradient fractions using the QIAamp Viral RNA kit as described by Qiagen. Before starting, the Carrier RNA was resuspended in 310 μl Buffer AVE. A mixture of 560 μl Buffer AVL and 5.6 μl Carrier RNA-AVE was made for each fraction (for a complete gradient, 11.76 ml Buffer AVL and 117.6 μl Carrier RNA-AVE). In a 1.6 ml tube, 560 μl of the Buffer AVL/carrier RNA-AVE mixture was added to 140 μl of unconcentrated gradient fraction. The samples were mixed by vortexing for 15 sec and incubated for 10 min at room temperature. Followed by the addition of 560 μl of 100% ethanol to each tube, mixed by pulse vortexing, and briefly centrifuged. The sample was added to the column on the vacuum manifold in two successive 630 μl aliquots. The column was washed with 750 μl Buffer AW1, then 750 μl of AW2. The columns were placed into collection tubes and centrifuged (21,000 x*g*) for 1 min to dry the membrane. The columns were transferred to 1.6 ml tubes, 60 μl of Buffer AVE was added to each column, incubated at room temperature for 1 min, and centrifuged for 1 min at 6,000 x*g* to elute the RNA. Recovered RNA was stored at -20°C until further use.

Prior to Reverse Transcriptase-PCR (RT-PCR), the RNA samples were treated with TURBO DNA-*free* (Ambion). Briefly, in a 0.6 ml tube, 50 μl of RNA sample, 0.1 volumes (5 μl) of 10X TURBO DNase Buffer and 1 μl of TURBO DNase were gently mixed, then incubated at 37° C for 20-30 min. 0.1 volumes of resuspended DNase

Inactivation Reagent were added, the tubes were incubated for 2 min at room temperature, while occasionally mixing by flicking the tube. The inactivation reagent was pelleted by centrifugation at 10,000 x*g* for 1.5 min and the RNA transferred to a new 1.6 ml tube. The DNA-free RNA was stored at -20°C until used for RT-PCR.

Detection of vRNA by relative quantitative real-time RT-PCR

Reverse transcription reactions were assembled on ice. Each 20 μl reaction contained: 7.4 μl distilled water, 10 μl 2X Sybr Green RT-PCR Reaction Mix (BioRad), 250 nM NL919 primer, 250 nM cNL1054 primer and 0.4 μl iScript Reverse Transcriptase for One-Step RT-PCR (Bio-Rad), and 2 μl of DNA-free RNA sample. The vDNA PCR standards of diluted pNLX plasmid (described above) were measured in triplicate to generate a standard curve. For these reactions, the mix did not contain iScript Reverse Transcriptase since the standards were DNA. The plates were covered with flat top caps, cut, and briefly centrifuged as described above. Real-time RT-PCR was performed in an iQ5 Multicolor real-time PCR detection system (Bio-Rad). The program parameters were: an initial annealing/RT extension at 50°C for 10 min; denature at 95°C for 30 sec; 95°C for 5 min; followed by 45 cycles of: 1) denaturing at 95°C for 20 sec, 2) annealing at 55°C for 20 sec, and 3) extension with real-time capture at 72°C for 30 sec; final denaturing at 95°C for 1 min; and annealing at 55°C for 30 sec, ending with a melt curve of 81 cycles at 55°C – 95°C for 10 sec.

***In vitro* integration assay**

PIC lysates were thawed on ice and treated with 20 μg/ml RNaseA (Qiagen, Valencia, CA) for 10 min at room temperature prior to integration reactions. The reactions were carried out in a 1.6 ml tube in a final volume of 350 μl. Water (26.5 μl or 30 μl with and without target reactions respectively) and 70 μl 5X Integration Reaction Buffer (final concentrations of 20 mM HEPES (pH 7.4), 150 mM KCl, 1 mM $MgCl_2$, 4% glycerol, 5 mM DTT) were added to the tube first, followed by 250 μl lysate or concentrated gradient fraction. Lastly, pTZ19R target DNA (Fermentas, Glen Burnie, MD) was added to the plus target samples to a final concentration of 3 ng/μl. The reaction mix was allowed to sit on ice for 5 min, then incubated for 45 min at 37°C. Reactions were stopped by the addition of 6.08 μl 0.5M EDTA (final concentration 8 mM). Reactions were deproteinized by the addition of 19 μl 10% SDS (0.5% final concentration) and 9.5 μl of 20 mg/ml Proteinase K (0.5 mg/ml final concentration; Invitrogen) for 1.5 hr at 56°C. DNA was isolated by a phenol extraction followed by two phenol:chloroform extractions and ethanol precipitation. Briefly, samples were mixed with 1 volume of saturated phenol (Ambion) in 1.6 ml tubes. The tubes were mixed by rotating at 4°C for 5 min and the phases separated by centrifugation at 21,000 x*g* for 5 min. The aqueous phase was transferred to a new 1.6 ml tube and the samples extracted twice by same rotation and centrifugation process with 1 volume phenol:chloroform:IAA (Ambion). The final aqueous phase was transferred to a new 1.6 ml tube containing 36.5 μl 3 M sodium acetate (0.3 M final concentration) and 1 μl of GenElute LPA (Sigma Aldrich, St. Louis, MO). Two and a half volumes of 100% ethanol were added to the samples and DNA precipitated O/N at -80°C. Samples were centrifuged at 21,000 x*g* for 15 min, the supernatant removed, and DNA pellet washed with 150 μl of 70% ethanol. DNA was re-centrifuged at 21,000 x*g* for 15 min, and the

ethanol removed. Pellets were air-dried 5 – 10 min, resuspended in 20 μl Tris-EDTA, and stored at -20°C.

Construction of pTZ19R-LTR standard

To construct a quantitative standard for the integration reactions, a HIV-1 LTR was cloned into pTZ19R vector backbone (Fermentas). The digestion of 21 μg pTZ19R was performed in a 100 μl volume with 5 μl *Pst*I and 5 μl *Bam*HI (New England BioLabs, Ipswich, MA) in 1X BSA and 1X Buffer 3 at 37°C for 4 hr. The digested vector was purified using a PCR purification kit (Invitrogen) as described by the manufacturer, and dephosporylated in an 80 μl reaction containing 50 μl plasmid vector, 1X Buffer, and 8 μl Calf Intestinal Alkaline Phosphatase (CIAP; Invitrogen) for 1 hr at 37°C. The digested and dephosporlated plasmid vector was purified by electrophoresis though 1% SeaPlaque GSG Agarose (Lonza, Allendale, NJ) containing 5 μg/ml ethedium bromide. The DNA was visualized by ultraviolet light and the digested vector excised with a clean razor blade. The DNA was extracted from the gel using the QIAquick Gel Extraction Kit (Qiagen) according to the manufacturer's protocol. Briefly, the gel slices were transferred to a 5 ml polystyrene round bottom tube and weighed. Three volumes of Buffer QG were added to the tube and the mixture incubated at 50°C. The tube was incubated for 10 min, inverting every 2 min, until the gel slice was no longer visible. One gel volume of isopropanol was added to the tube, and inverted to mix. To capture DNA, the entire sample was added to the silica column, under vacuum pressure, in increments of 800 μl. The column was washed with 0.5 ml Buffer QG and 0.75 ml Buffer PE. The column was transferred to 1.5 ml tube and excess wash buffer was removed by centrifugation for 1 min at 10,000 x*g*, then transferred to a new 1.5 ml tube and the

plasmid vector eluted with 50 μl of Buffer EB, pre-warmed to 65°C. The column was incubated at room temperature for 1 min and the restricted vector was subsequently recovered by centrifugation for 1 min at 10,000 x*g*.

To create the insert, the single HIV-1 LTR DNA was amplified from pNLX template in eight 50 μl PCR reactions. Each reaction included 2 ng NLX, 1X Biomix Red (BioLine, Taunton, MA), 250 nM of primers NL1-BH1 and cNL702Pst1 (Table 1). PCR parameters were: initial denaturation at 95°C for 4 min; followed by 24 cycles of: 1) denature at 95°C for 20 sec, 2) annealing at 50°C for 30 sec, and 3) extension 72°C for 90 sec; and final extension for at 72°C for 2 min. After amplification the HIV-1 LTR DNA insert was gel purified as described above.

A pre-ligation gel on 1% GenePure LE (ISC BioExpress, Kaysville, UT) was used to compare the DNA concentration of plasmid vector backbone and the insert. A 10 μl ligation reaction was assembled on ice in 0.6 ml tubes containing approximate equivalent molecular ratios of the restricted vector and the insert, 1X Buffer and 1 μl T4 ligase (HC) (Invitrogen). The reaction was incubated overnight in a 14°C water bath. Chemically competent α-select *E. coli* cells (BioLine) were transformed using 4 μl of the ligation reaction as described by the manufacturer. The tubes containing the bacteria and ligation reaction were incubated on ice for 30 min, heat shocked in a 42°C water bath for 45 sec, and returned to ice for 2 min. Then, 950 μl of SOC (New England BioLabs) media was added and the tubes placed in a 37°C shaking incubator (250 rpm) for 1 hr. The cells were plated on LB+ampicillin plates (100 μl/ml) and incubated overnight at 37°C.

Plasmid DNA mini-preps were performed on randomly selected clones from the plates. Each colony was grown in a 3 ml culture of LB+ampicillin media and incubated

overnight at 37°C in a shaking incubator (250 rpm). Plasmid DNA was isolated using a plasmid purification kit as described by the manufacturer (Qiagen). Briefly, the cells were centrifuged at 6,800 x*g* for 3 min, media discarded and the cells resuspended in 250 μl of Buffer P1 (with RNase A added). The resuspension was transferred to a 1.6 ml tube, and 250 μl Buffer P2 and lysis buffer were added to the tube. The suspension was mixed by inverting the tube 5 times and incubated at room temperature for 5 min. 350 μl of Buffer N3 was added, mixed by inverting vigorously 5 times and incubated on ice for 5 min. The cellular debris was removed by centrifuging the tubes at maximum speed (18,000 x*g*) for 10 min at 4°C. Each supernatant was added to a QIAprep spin column. The sample was centrifuged for 1 min, washed with 0.5 ml Buffer PE and re-centrifuged. The flow through was discarded after each centrifugation. Residual wash buffer was removed by centrifuging the column for an additional 1 min. The column was transferred to a new 1.6 ml microcentrifuge tube to collect the DNA. The DNA was eluted by centrifugation with 50 μl Buffer EB (pre-warmed to 65°C), after 1 min of incubation at room temperature. The DNA was stored at -20°C until further use.

Clones were assessed by restriction endonuclease mapping followed by PCR screening. Plasmid DNA (1 μl) was digested with *Bgl*II (New England BioLabs) in a 10 μl reaction containing 1 μl Buffer 3 and 0.5 μl *Bgl*II. Positive clones were identified by the presence of a 3.5 kb band on agarose gel. The PCR screening was done in a 25 μl reaction on 2 μl DNA diluted 1:200 from the miniprep DNA. The reaction contained 2X Bioline, 250 nM of primers NL1 and cNL702. The program parameters were: initial denaturing at 95°C for 4 min; followed by 24 cycles of: 1) denaturing at 95°C for 20 sec, 2) annealing at 50°C for 30 sec, and 3) extension at 72°C for 90 sec; and a final extension at 72°C for 2 min.

Clones with correct insert ligation were confirmed by DNA sequence analysis. The 12 μl sequencing reaction containing 2 μl plasmid DNA, 1.3 μl T7 primer and 2.4 μl Big-Dye Terminator v3.1 (1X final concentration; Applied Biosystems, Foster City, CA). Sequencing parameters were: initial denaturization at 95°C for 5 min; followed by 60 cycles of: 1) 96°C for 10 sec and 2) 50°C for 4 min. The reactions were purified and sequenced by the Creighton University Molecular Biology Research Core Facility.

Detection of integrated products from in vitro integration assay by nested PCR

A schematic diagram of the nested PCR strategy to measure integration activity is shown in Figure 1. The first PCR mix was assembled on ice. Reactions were performed in round-top PCR strip tubes. A single 20 μl reaction contained: 14.6 μl distilled water, 2 μl 10X iTaq buffer (1X final concentration, Bio-Rad), 1 mM $MgCl_2$, 1 mM dNTPs (Bio-Rad), 250 nM pTZ2414 primer, 250 nM pTZ2413 primer, 250 nM L-653 primer 0.1 μl iTaq DNA pol (Bio-Rad), and 2 μl of DNA or PCR standards. The tubes were centrifuged briefly and the PCR amplification performed using a Mastercycler (Eppendorf, Westbury, NY). The program parameters were: initial denaturing at 95°C for 15 min; followed by 18 cycles of: 1) denaturing at 94°C for 30 sec, 2) annealing at 58°C for 20 sec, and 3) extension at 72°C for 4 min; and a final extension at 72°C for 10 min. After the first PCR, the reactions were diluted 1:1000 in distilled water prior to the quantitative PCR ($_Q$PCR). Each $_Q$PCR reaction of 20 μl contained: 7.8 μl distilled water, 10 μl 2X SYBR Green (1X final concentration, Bio-Rad), 250 nM Linker Primer, 250 nM NL506 primer, and 2 μl of the 1:1000 diluted first PCR reaction. Each sample was assayed in triplicate for the nested $_Q$PCR. The real-time PCR was performed using an iQ5 Multicolor real-time PCR detection system (Bio-Rad). The program parameters

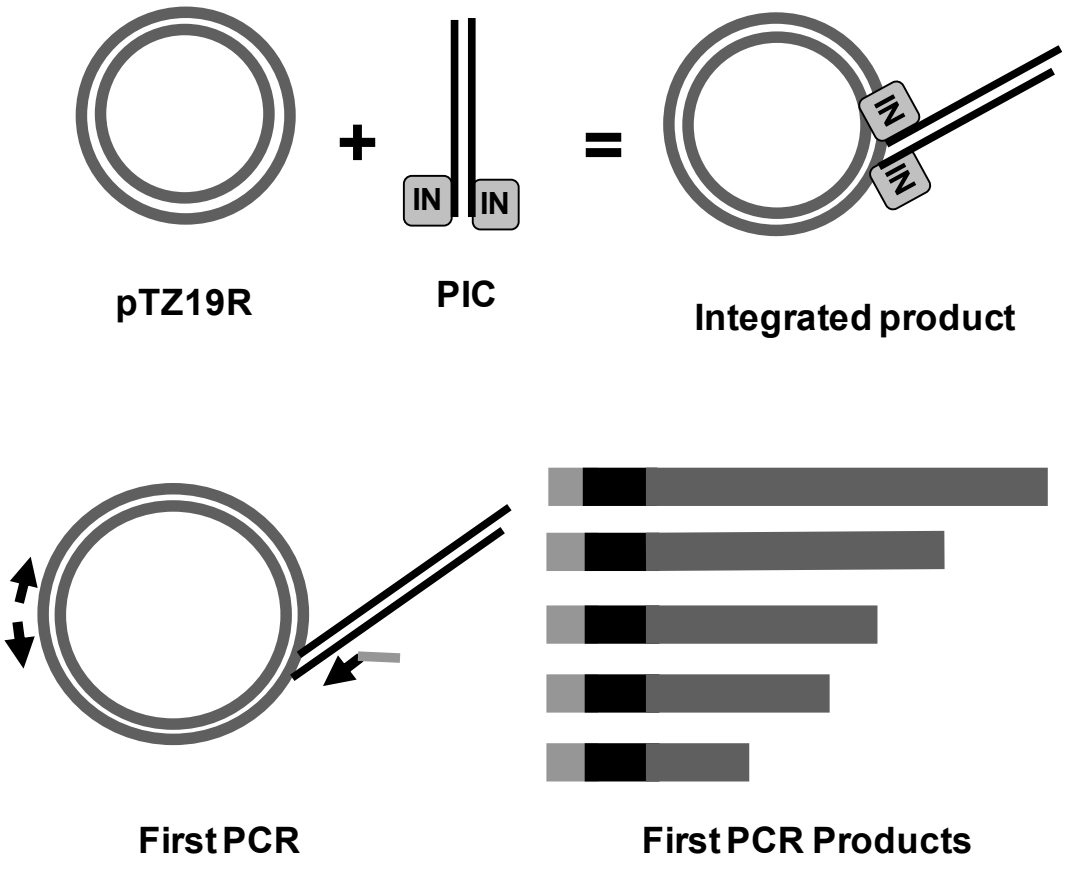

Figure 1. Diagram of nested quantitative real-time PCR for detection of integration products. When the pTZ19R and PIC are mixed during the integration assay, integrated products are formed. These integrated products are amplified in the first PCR by an HIV-1 primer with a linker, and back to back plasmid primers to yield the first PCR products. The products are detected by real-time PCR using the linker primer and an internal HIV-1 primer (primers listed in Table 1).

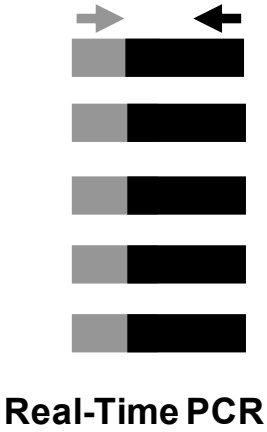

were: initial denature step at 95°C for 6 min; then 40 cycles of: 1) denaturing at 95°C for 20 sec, 2) annealing at 58°C for 20 sec, 3) extension at 72°C for 30 sec (real-time capture); followed by a final denature step at 95°C for 60 sec, and extension for at 60°C for 60 sec; and finally a melt curve analysis of 31 steps from 60°C – 91°C.

Detection of reverse transcriptase (RT) activity by enzymatic incorporation assay

RT activity was determined from each gradient fraction by an enzymatic [^{32}P] TTP incorporation assay (Belshan et al. 2009, 178-184; Goff, Traktman, and Baltimore 1981, 239-248; Willey et al. 1988, 139-147). The 100 μl reaction mixture contained: 50 mM Tris, pH 7.9, 75 mM KCl, 2 mM DTT, 0.1875 mM ATP, 5 mM $MgCl_2$, 25 mg/ml RT Primer, 0.05% NP-40, and 0.112 μCi [^{32}P]-α-TTP. The reactions were carried out in triplicate containing 20 μl of each fraction and 75 μl of the reaction mixture in 96-well round bottom plates. The plate was covered with plate sealing tape, placed in an acrylic glass case and incubated overnight at 37°C. The next day, 90 μl was transferred to a Multiscreen DE plate on a Multiscreen manifold system (Millipore). The vacuum was applied between 5 and 8 mm Hg to capture incorporated DNA. The vacuum was removed and seal broken by slightly picking up the plate. The plate was washed 5 times with 200 μl 2X SSC (0.3 M NaCl, 0.03 M sodium citrate, pH 7.0). In between each wash the vacuum was turned off and the seal broken. A final wash of 200 μl 95% ethanol was added to dry the membranes. Once dry, the back of the plate was removed carefully, the filters punched out with forceps and transferred to scintillation vials with 2 ml of ScintiSafe Econo 2 (Fisher Scientific). Samples were measured using a LS 6500 Multi-purpose Scintillation Counter (Beckman Coulter, Fullerton, CA) with an efficiency of 95.8%.

Detection of capsid (CA) by ELISA

CA was measured using a HIV-1 p24 Antigen Capture Assay (Advanced BioScience Laboratories, Inc, Kensington, MD) according to protocol. The standards were diluted from the standard stock to 100, 50, 25, 12.5, 6.25 and 3.1 pg/ml. When assaying gradient fractions, fractions 1 – 4 were diluted 1:500 and fractions 5 – 20 and pellet were diluted 1:100 in PBS. When measuring virus stock concentration, the virus stocks were diluted 1:50,000 in PBS. Briefly, all contents of the kit were warmed to room temperature before use. First, 25 μl of Disruption Buffer were added to each well, then either 100 μl of sample, standard, or PBS (blank) were added. The plate was gently tapped to mix, covered with a Plate Sealer and incubated at 37°C for 1 hr. The samples were aspirated and the wells washed five times using a Nunc-Immuno Wash 8 (Thermo Scientific). After the last aspiration, the plate was inverted and tapped to remove any residual liquid. Next, 100 μl of Conjugate Solution was added to each well and the plate covered and incubated for 1 hr at 37°C. The samples were aspirated and the wells washed as described above. Finally, 100 μl of peroxidase substrate was added to each well and the plate incubated uncovered for 30 min at room temperature. 100 μl of the Stop Solution was added to the wells in the same order the peroxidase substrate. The absorbance values were measured at 450 nm using a VersaMax plate reader (Molecular Devices, Sunnyvale, CA) set to pre-mix the plate for 3 sec.

Detection of matrix (MA) by Western blot detection

A sample from each concentrated gradient fraction was mixed with 1 volume of 2X sample buffer (2% SDS, 0.0125 M NaH_2PO_4, 20% glycerol, 0.11 M 2-mercaptoethanol, 0.1 M DTT, 0.024% Bromophenol Blue) and boiled for 5 min. A 15%

Acrylamide SDS-Poly acrylamide Gel Electrophoresis at a constant current of 100 V was used to separate 25 μl of sample from each fraction. Proteins were transferred to PVDF membranes (Millipore) using a semi-dry blotter and wetted blotting pads (Bio-Rad) cut to the size of the gel. Briefly, the PVDF membranes were pre-wetted with 100% methanol for 1 min, and both the membranes and gels equilibrated in Transfer Buffer (10 mM CAPS, 10% methanol, pH 11.0) for 15 min with shaking. The Blotting Pads were briefly wet in Transfer Buffer and the transfer assembled as described by the manufacturer (Bio-Rad). The proteins from the mini-gels were transferred for 35 min at a constant 100 mA, or Criterion gels were transferred for 45 min at a constant 360 mA. After transfer, the PVDF membranes were removed and air-dried overnight.

Membranes were blocked with 1% dry milk in TBS-T (50 mM Tris pH 7.5, 150 mM NaCl, 0.04% Tween-20) by rocking gently for 10 min at room temperature. The blocking solution was removed and blots washed twice for 10 min with TBS-T using vigorous rocking. The primary α-MA (a kind gift from Lee Ratner) antibody was used at a 1:2000 dilution in TBS-T and incubated with the blot for 30 min with gentle rocking. The primary antibody was removed and the blots washed with TBS-T 3 times for 10 min with vigorous rocking. The blots were then incubated with secondary antibody (HRP-conjugated donkey-α-rabbit; GE Healthcare (Waukesha, WI)) diluted 1:7500 in TBS-T for 30 min with gentle rocking. The secondary antibody was removed and the membrane washed vigorously 4 times with TBS-T for 10 min and twice with TBS. Bands were detected by chemiluminescence using ECL reagent as described by the manufacturer (Pierce, Pittsburg, PA). The membranes were removed from the TBS; excess wicked away with a paper towel, the blots placed face up on Saran wrap, and covered with ECL reagent for 5 min. Excess ECL was removed and the membrane sealed with Saran wrap. The blot was exposed to film (5 sec – 5 min) in a dark room.

Images were acquired by flat-bed scanning and adjusted for brightness/contrast if necessary using Adobe Photoshop.

Results

Chapter 1:

Purification of HIV-1 preintegration complexes by velocity gradient centrifugation.

Optimizing infection methods to produce preintegration complexes.

There is no consensus regarding the optimal length of infection to produce preintegration complexes (PICs) in the literature. Our initial studies set out to determine the ideal infection parameters to maximize PIC production, including virus pseudotyping, cell type, and infection length. The level of infection was measured by quantifying the amount of viral DNA (vDNA) present in cell lysates by quantitative real-time PCR using HIV-1 *gag* specific primers (Table 1). To confirm that the exogenous plasmid DNA used to generate virus stocks did not contribute to the level of vDNA in infection assays, cells were infected with heat inactivated (H.I.) virus as a negative control (Figure 2A). As expected, no vDNA was detected in the HI virus infections, indicating an absence of contaminating vDNA. HIV-1 pseudotyped with vesicular stomatitis virus (HIV+VSVg) is typically used to produce high levels of nucleoprotein complexes (NPCs) (Bukrinskaya et al. 1998; Arfi et al. 2009; Arhel et al. 2006; McDonald et al. 2002; Limon et al. 2002) since infection with wild-type HIV-1 does not produce high levels of PICs in cell culture. First, we compared the level of infection between wild type and HIV+VSVg pseudotyped virus in SupT1 cells (Figure 2A). HIV+VSVg contained 16-fold more vDNA than wild type virus corroborating previous studies that VSVg-pseudotyped HIV-1 results in a more efficient infection compared to wild-type HIV-1. Second, we compared the

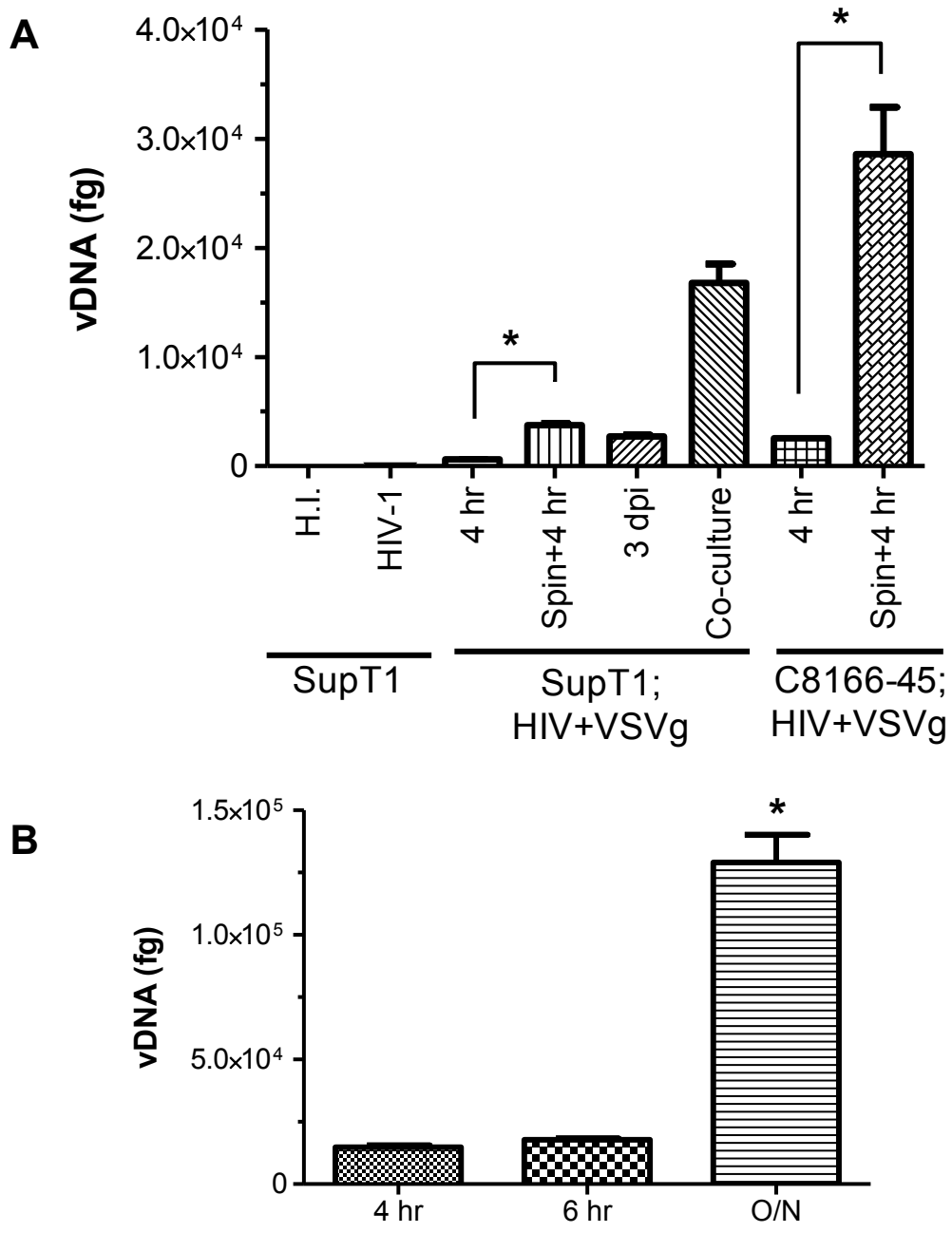

Figure 2. Optimization of infection method. A sample was removed and DNA extracted and the levels determined by quantitative real-time PCR using HIV *gag*-specific primers. **A.** SupT1 or C8166 cells were infected as indicated. **B.** C8166-45 cells infected via spinoculation and cultured for lengths listed. H.I., heat inactivated; HIV+VSVg, pseudotyped virus; Spin, spinoculated; 3 dpi, 3 days post infection; 4 hr and 6 hr, culture length post spinoculation; O/N, overnight; $p \leq 0.005$ (unpaired Student's T test). Representative of at least three independent experiments. Error bars indicate standard deviation of triplicate real-time PCR samples.

infectivity of two T-cell lines, SupT1 and C8166-45, using HIV+VSVg pseudotyped virus (Figure 2A). C8166-45 cells produced a 4-fold higher level of infection compared to SupT1 cells in 4 hr infections. Third, we investigated whether spinoculation (the application of centrifugal force to increase virus-cell interaction) would enhance the production of PICs. Spinoculation has been reported to improve efficiency of HIV infection up to 40-fold in another T-cell line, CEM-SS (O'Doherty, Swiggard, and Malim 2000). We measured the effect of spinoculation for both SupT1 and C8166-45 cells using HIV+VSVg virus. The cells were centrifuged at 25°C for 2 hr and 1050 x*g,* prior to incubation at 37°C. As shown in Figure 2A, spinoculation increased infection of SupT1 cells 6-fold and C8166-45 cells 11-fold compared to the non-spinoculated infections ($p \leq 0.005$, unpaired Student's t-test). Similar to the non-spinoculated infections, spinoculation of the C8166-45 cells resulted in a 7-fold higher infection compared to the spinoculation of SupT1 cells.

Infection by co-culture with acutely infected cells is another method that has been used to obtain high levels of infection and produce PICs (Sato et al. 1992; Karageorgos, Li, and Burrell 1993). We investigated the efficiency of infection using the co-culture method with SupT1 cells. Cells were infected with HIV+VSVg pseudotyped virus, and propagated until syncitia were visible (~3 days). These acutely infected cells were co-cultured with uninfected SupT1 cells at a ratio of 1:3 for 4 hr. vDNA levels were determined for both acute and co-cultured infections. The cells infected by co-culture had a 6-fold higher level of vDNA compared to acutely infected cells, but did not reach the level of infection achieved by infecting C8166-45 cells via spinoculation with HIV+VSVg virus (Figure 2A).

Although most previously published studies utilized a short infection length (2-4 hr; Fassati and Goff 2001; Farnet and Haseltine 1991; Farnet and Haseltine 1990) to

produce PICs, a few studies have reported that longer culture lengths result in an increased production of PICs (Bukrinsky et al. 1993; Heinzinger et al. 1994). As our final investigation for the optimal infection methods, we determined the length of incubation after spinoculation that resulted in the highest level of infection. C8166-45 cells were infected by spinoculation and cultured for 4 hr, 6 hr, or overnight (O/N, ~20 hr; Figure 2B). In contrast to many published studies, only relatively low levels of vDNA were recovered from 4 hr and 6 hr infections. The level of infection increased over 10-fold when the infection was cultured O/N. Combined, these studies demonstrate that the highest levels of infection are achieved by overnight infection of C8166-45 cells with HIV+VSVg by spinoculation.

Detection of preintegration complexes using an *in vitro* integration assay.

The PIC is operationally defined by its ability to integrate vDNA into a heterologous target DNA *in vitro* (Brown et al. 1987). Integration assays were performed and the activity quantified using the protocol described in *HIV Protocols* (Engelman 2009) with several modifications as described in Materials and Methods and Belshan et al.(2009). Notably, 1) circular pTZ19R was used as a target, 2) the reactions were carried out in the presence of an integration reaction buffer, 3) PICs were produced and harvested from infected C8166-45 cells using a mild detergent lysis (0.1% Triton X-100 in buffer K), and 4) the nested quantitative real-time PCR assay used to measure the level of vDNA integration into the target plasmid utilized a plasmid DNA standard to permit inter-experiment comparison between samples.

Several integration reactions were performed to demonstrate the specificity of our assay. For each sample two reactions, one with (plus) and one without (minus)

target plasmid, were performed. The detection of high levels of integrated products detected in the plus target reaction compared to low levels in the minus target reaction demonstrated specific PIC activity in infected lysates (Figure 3). To confirm the efficacy of the assay we also performed several control reactions (Figure 3). Near background levels of integration occurred when reactions were held on ice, which were significantly lower than the reaction with target control ($p \leq 0.005$, unpaired Student's t-test). There was an absence of integrated products detected in buffer only (no lysate) and uninfected cell lysate with or without target. Infected cell lysates from cells treated with nevirapine, an RT inhibitor, displayed only background levels of integration and were significantly lower than the plus target reaction ($p \leq 0.005$, unpaired Student's t-test).

Raw data from real-time PCR is in Figure 4. The amplification curve is shown in Figure 4A. A standard curve was generated from the standards with the samples plotted on the curve (Figure 4B). After amplification, a melt curve and melt peak was used to analyze the products (Figure 4C and D). The melt curve and melt peak were the same for all products, so only one product was amplified. To further ensure our assay detected one product, the products of real-time PCR were visualized on agarose gel (Figure 4D subset). Only one band was detected in the products from the highest standard (1000 fg) and no bands were detected in the water control. Taken together this demonstrates that only one product was amplified and detected by the PCR assay.

O/N infections produce the highest levels of preintegration complexes.

We determined that C8166-45 cells infected O/N via spinoculation with HIV+VSVg pseudotyped virus had the greatest infection efficiency as measured by vDNA levels. To investigate the optimal harvest time for active PICs we performed

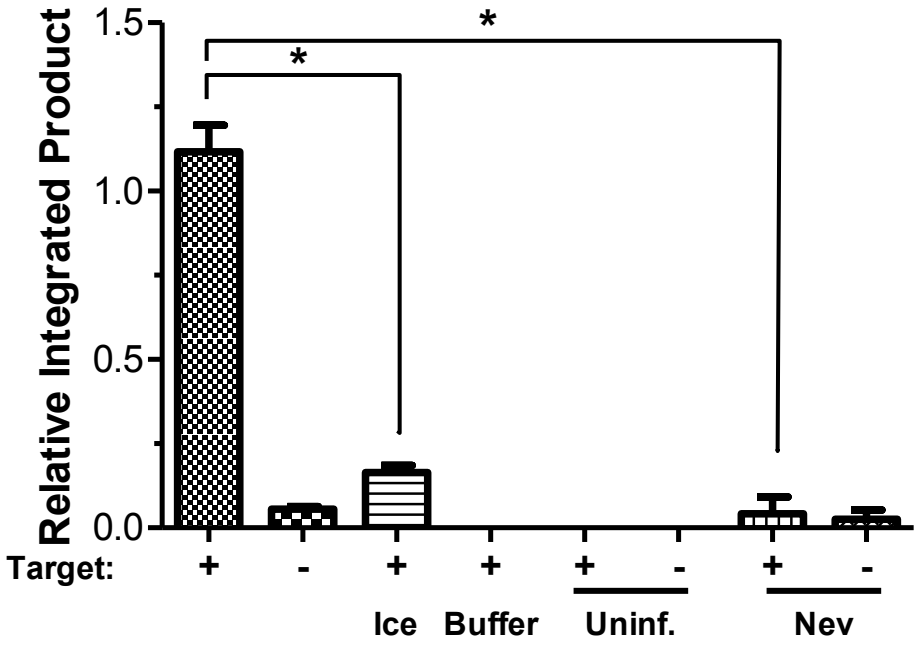

Figure 3. Integration assay validation. PIC lysates were tested for integration activity. Relative integration products were measured by quantitative real-time PCR (fg). +, reaction with target; -, reaction without target added; Ice, reaction kept on ice; Buffer, no lysate/buffer control reaction; Nev, PIC lysates produced from cells treated with nevirapine (20 μM final concentration) during infection; Uninf., uninfected cell lysate; *, $p \leq 0.005$ (students T test). Representative of at least three independent experiments. Error bars represent standard deviation from triplicate real-time PCRs.

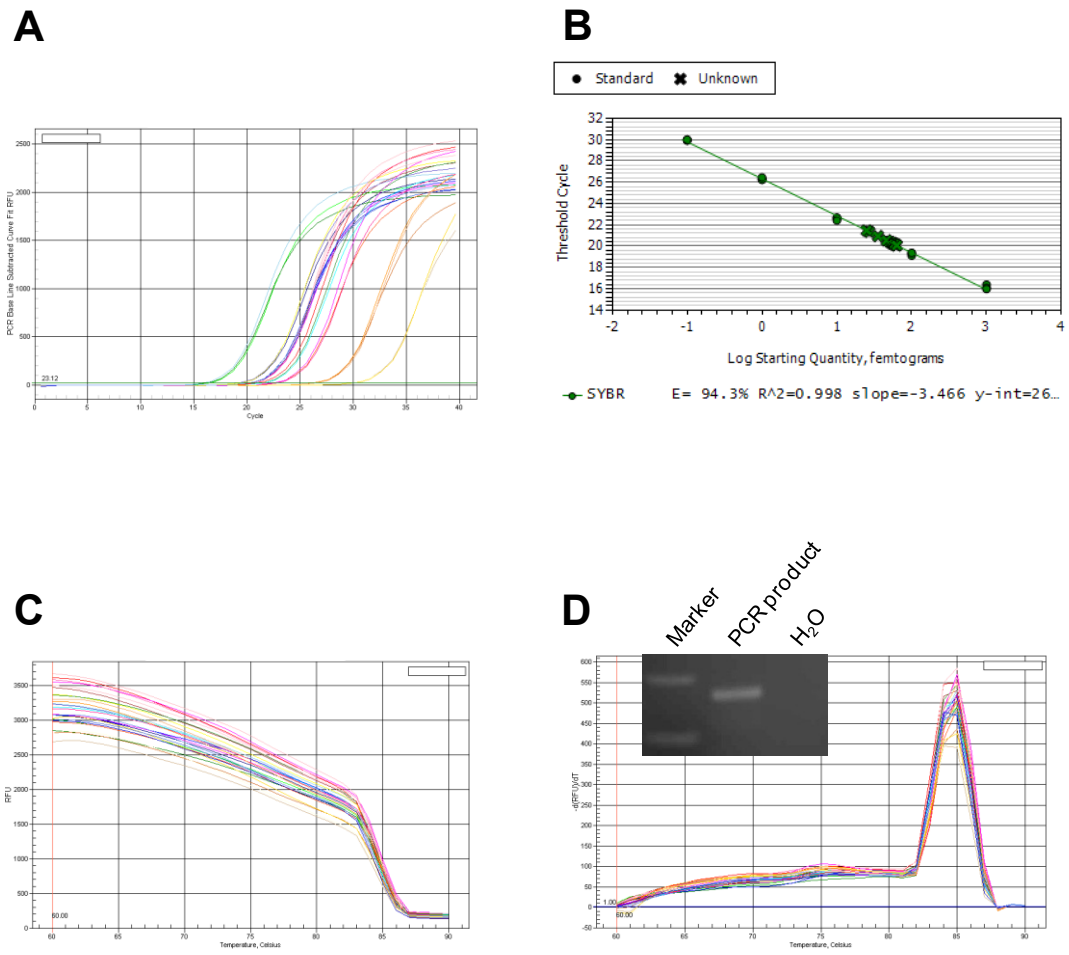

Figure 4. Integration assay validation. Data from integration assay PCR. **A.** Amplification curve of real-time PCR. **B.** Standard curve generated from real-time PCR with unknowns plotted against the curve. **C.** Melt curve chart of real-time PCR products. **D.** Melt peak of real-time PCR products. Subset is the products from real-time PCR separated by 2% agarose gel. Curves representative of more than 10 independent experiments.

another series of time course infections and analyzed the amount of integration activity produced from 4 hr, 6 hr, and O/N infections (Figure 5). Correlating with the vDNA experiments, the 4 hr and 6 hr infections produced similarly low, but detectable levels of integration activity. In comparison, the O/N infections produced lysates with 10-fold higher levels of integration activity than those obtained from 4 hr or 6 hr infections. Together with the vDNA analysis these results confirm that the maximum levels of integration activity and therefore PICs are produced from O/N infections.

Velocity gradient centrifugation partially purifies five vDNA complexes.

Gradient centrifugation can be used to separate and purify molecules by size or density. Velocity gradient centrifugation (VGC), also known as rate-zonal centrifugation, is the separation of molecules by size. This separation is achieved using a short length of centrifugation in which the sedimentation of molecules is primarily determined by hindrance of their movement as the viscosity of the medium increases. As the length of centrifugation increases (equilibrium centrifugation), molecules will eventually reach an equilibrium with the gradient medium and hence, separate by density (Figure 6). We explored the VGC method to separate and partially purify HIV-1 NPCs. Several concentrations of sucrose and ultracentrifugation lengths were assayed for their capacity to separate NPCs (data not shown). We determined that gradients of 5-45% (w/v) sucrose in Buffer K were appropriate to purify HIV-1 NPCs. After ultracentrifugation, the gradients were fractionated using the Biocomp gradient station to yield 20 fractions (~0.6 ml) plus the pelletable material (recovered by resuspending with 0.6 ml Buffer K). The linearity of gradients was monitored by measuring the refractive index of each fraction (an example is shown by the gray line in Figure 7).

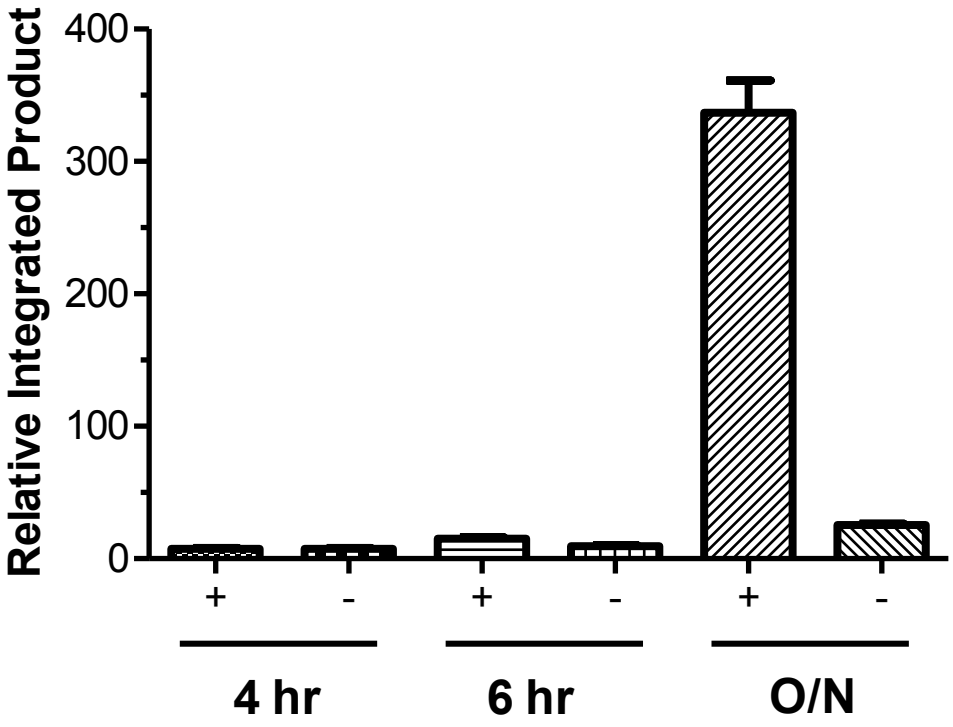

Figure 5. Optimal harvest time to recover active PICs. C8166 cells were infected for 4 hr, 6 hr, or overnight (O/N). PIC lysates were tested for integration activity. Relative integration products were measured by quantitative real-time PCR (fg). +, reaction with target; -, reaction without target. Representative of three independent experiments. Error bars represent standard deviation from triplicate real-time PCRs.

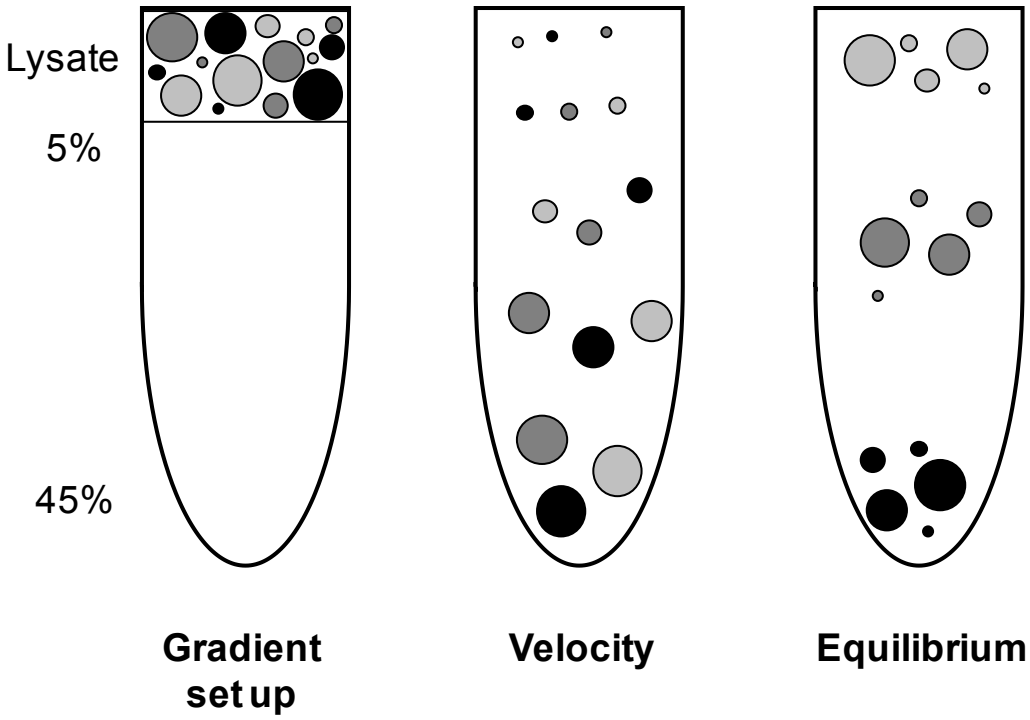

Figure 6. Principle of Velocity Gradient Centrifugation (VGC). Sample was layered to the top of 5-45% (w/v) sucrose in Buffer K(-) gradients. Velocity Gradient Centrifugation separates molecules by size. Equilibrium Gradient Centrifugation separates molecules by density.

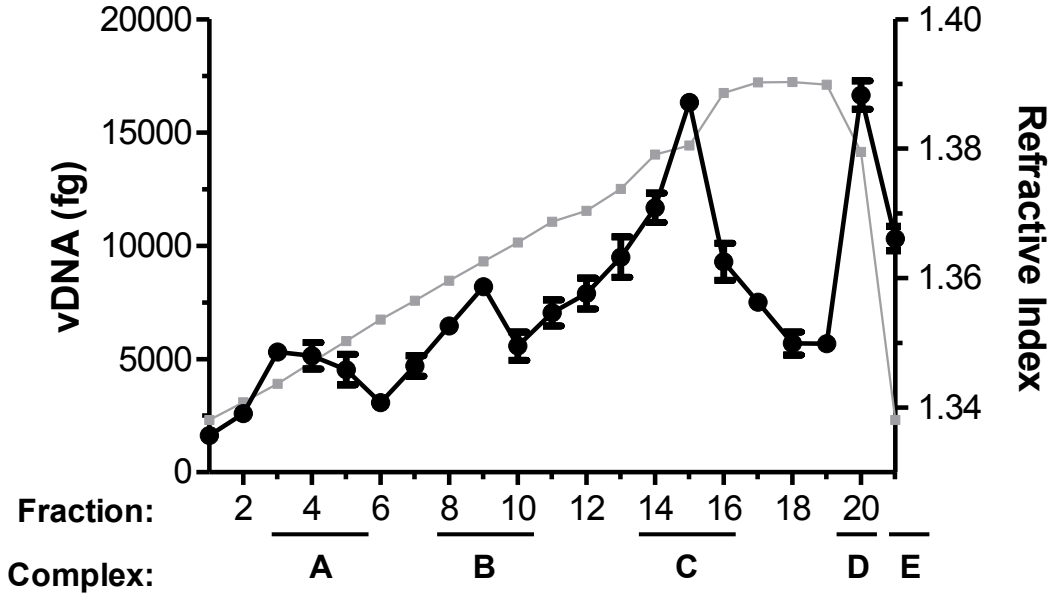

Figure 7. Distribution of vDNA in 5-45%/1 hr gradients. Fractions listed below graph; Complexes indicated below fractions; black circles, vDNA; gray squares, refractive index. Representative of at least 10 independent experiments. Error bars indicate standard deviation from triplicate real-time PCRs.

To detect vDNA-containing NPCs, DNA was isolated from each fraction and measured by quantitative real-time PCR using *gag*-specific primers (Figure 7). All fractions contained detectable levels of vDNA; however 5 complexes (lettered A through E from the top of the gradient) were consistently observed in gradients centrifuged for 1 hr at 207,000 x*g* (5-45%/1 hr). Complexes A (fractions 3 – 5) and B (fractions 8 – 10) were the peaks with the lowest concentration of vDNA. The majority of the vDNA was detected in Complex C, which consisted of fractions 14 – 16. Due to a variable amount of leakage that occurs during each fractionation, vDNA levels in Complex D (Fraction 20) and Complex E (the pellet) were inconsistent among replicate gradients. Typically the amount of vDNA in fraction 20 was higher than that in the pellet. VGC of uninfected cell lysates resulted in no detection of vDNA in any fractions (data not shown).

Complex C (Fraction 14 – 15) contains preintegration complexes.

To identify which complexes contain PICs, we tested the fractions comprising the 5 complexes for in vitro integration activity. Fractions of individual gradients did not contain measurable integration activity (data not shown). To overcome this, matching fractions from six gradients were combined and concentrated for each assay to a final volume of 650 μl using 5,000 MWCO ultrafiltration columns. As expected, the concentrated samples had 5-fold higher levels of vDNA compared to un-concentrated samples, a direct correlation with the total volume added (Figure 8), and the flow through contained no detectable levels of vDNA. Since levels higher than 5% sucrose resulted in decreased efficiency of DNA extracted by phenol and phenol:chloroform (data not shown), the samples were buffer exchanged by the addition of Buffer K, as described in

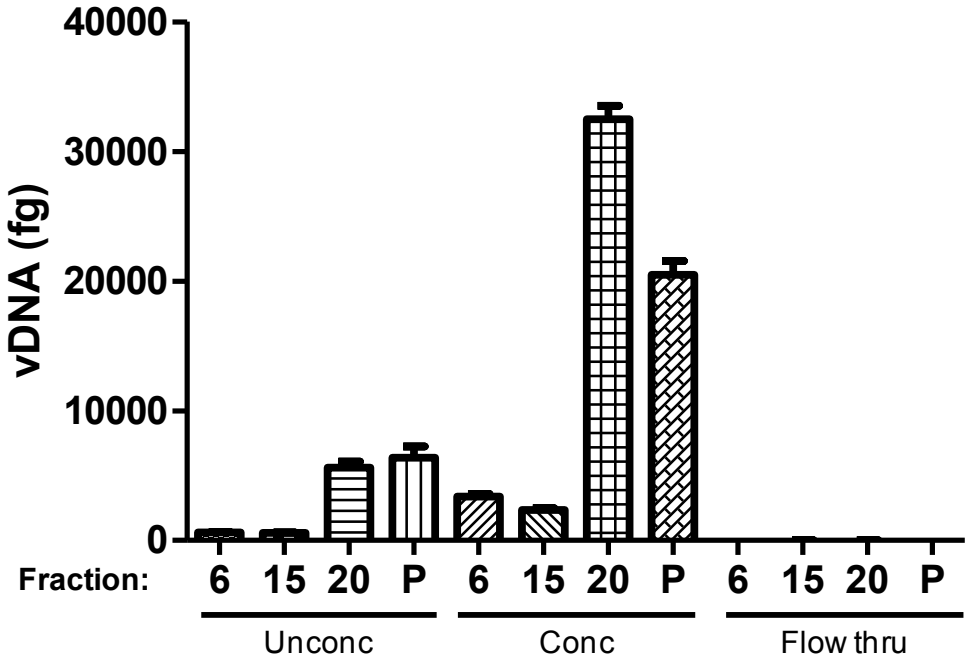

Figure 8. vDNA levels before and after centrifuge filter concentration. vDNA was extracted and levels were determined by quantitative real-time PCR. Unconc, unconcentrated fractions; Conc, concentrated fractions; Flow thru, discarded material not caught in the filter. Data from a single representative experiment. Error bars indicate standard deviation of samples assayed in triplicate.

methods, until the levels of sucrose were less than 5% as measured with a refractometer.

Since all fractions contained varying background levels of integration activity in control reactions without target, specific integration activity was calculated for each fraction by dividing the level of integration in the reaction with target by the corresponding control reaction without target. A value greater than one indicated specific integration activity in a reaction. The data in Figure 9 represents the average specific integration activity of the fractions that comprise each complex from a total of 4 individual experiments (e.g. Complex A is the combined average of fractions 3 – 5). The highest level of specific integration activity was detected in the fractions of Complex C, corresponding to the peak of highest vDNA. Specific integration activity was also detected in the fractions comprising Complex B, but less than those of Complex C ($p \leq 0.005$, unpaired Student's t-test). No specific integration activity was detected in the fractions contained in Complexes A, D or E, indicating these vDNA complexes were not PICs.

Reverse transcription complexes sediment distinctly from preintegration complexes.

It remains unresolved in the literature whether RTCs and PICs are distinct complexes. To investigate the sedimentation of RTCs in 5-45%/1 hr gradients, we first measured each fraction for viral RNA (vRNA), reverse transcriptase (RT) activity, and early reverse transcription product vDNA (ERT-vDNA). RNA was extracted from each fraction, DNase treated, and the relative amount quantified by quantitative real-time RT-PCR using *gag* specific primers. The sedimentation of vRNA was distinct from vDNA

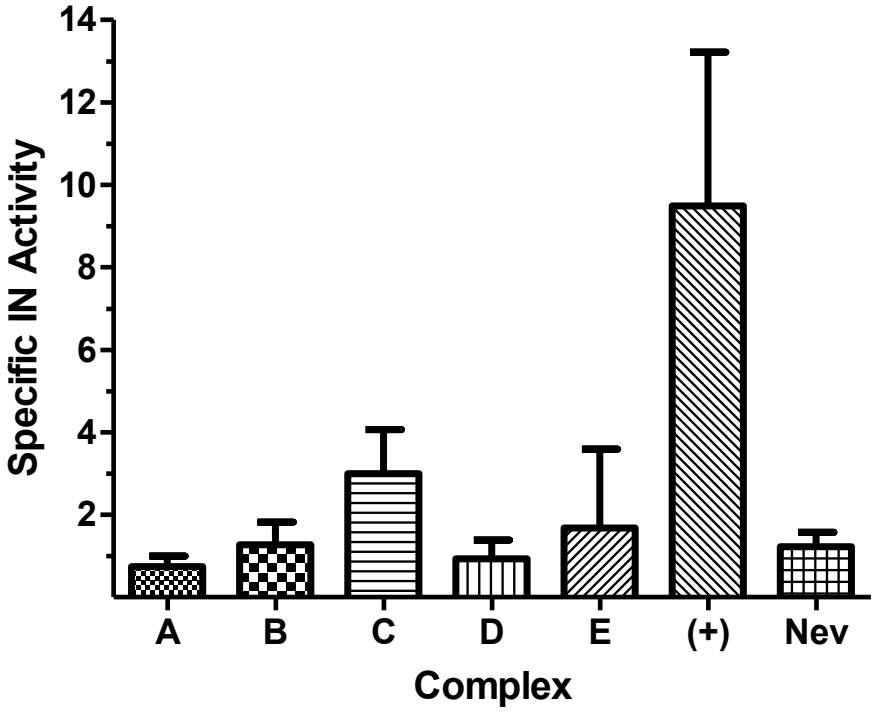

Figure 9. Integration activity of complexes in 5-45%/1 hr gradients. Specific integration activity determined by calculating the ratio of integrated products in reaction with target to reactions without target. A, B, C, D, and E, peak fractions from gradients; (+), unfractionated PIC lysate; Nev, Nevirapine treated PIC lysates. Error bars indicate standard deviation from at least three independent experiments.

(Figure 10A). The majority of vRNA sedimented to fractions 3 – 5, corresponding to the fractions of Complex A. Only low levels of vRNA were detected in the fractions that contained active PICs (Complexes B and C). Next, the level of RT activity in each fraction was determined using an enzymatic incorporation assay (Figure 10B; Goff, Traktman, and Baltimore 1981; Willey et al. 1988). Similar to the sedimentation of the vRNA, the majority of RT activity was detected in the fractions that correspond to Complex A, fractions 3 – 7, with amounts decreasing until fraction 12. Together the presence of vRNA and RT activity suggested that the RTCs sediment to fractions 3 – 7, or Complex A. To confirm that Complex A contains RTCs, we examined the distribution of ERT-vDNA. ERT-vDNA, or strong-stop DNA, is synthesized during the first step of reverse transcription and is present in the RTC. ERT-vDNA was detected using primers corresponding to the HIV-1 5' long terminal repeat (LTR; Figure 10C). Consequently, both early products and completed products of reverse transcription will be detected and, therefore, the distribution of peaks should be similar to Complexes B, C, D and E, but with an increase in vDNA levels in the presence of ERT. Similar to vRNA distribution, the highest level of ERT-vDNA was detected in the fractions of Complex A. Taken together these results support the conclusion that fractions 2 – 10 contain RTCs.

Capsid (CA) dissociates from nucleoprotein complexes purified by VGC.

CA has been reported to be at best only loosely associated with PICs during the early steps of HIV-1 infection (Bukrinsky et al. 1993; Farnet and Haseltine 1990; Fassati and Goff 2001). The distribution of CA in 5-45%/1 hr gradients was determined using a quantitative HIV-1 p24 Antigen Capture Assay. The majority of CA remained in the soluble, top fractions of the gradient (Figure 11) and did not migrate with vDNA or vRNA.

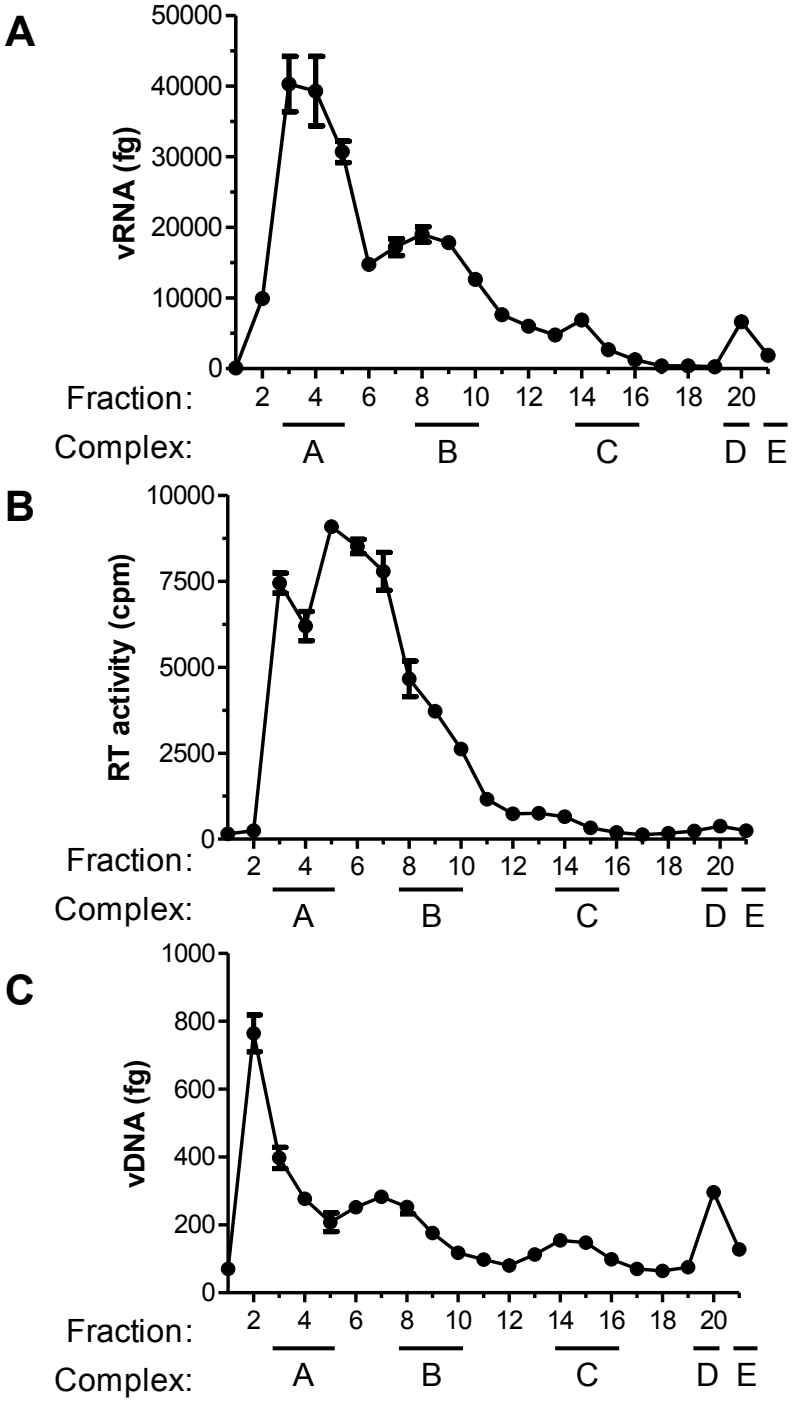

Figure 10. Distribution of RTC components in 5-45%/1 hr gradients. **A.** vRNA was isolated from each fraction using a viral RNA extraction kit. RNA was treated with Turbo DNA-*free* and the levels determined by quantitative real-time RT-PCR using *gag*-specific primers. **B.** The RT activity present in fractions was determined by in vitro [32P]TTP-incorporation assay. **C.** DNA was isolated from fractions and ERT-vDNA was detected using early RT product primers. Fractions listed below graph; Complexes indicated below fractions. Data is representative of at least three independent experiments, error bars indicate standard deviation from triplicate real-time PCRs.

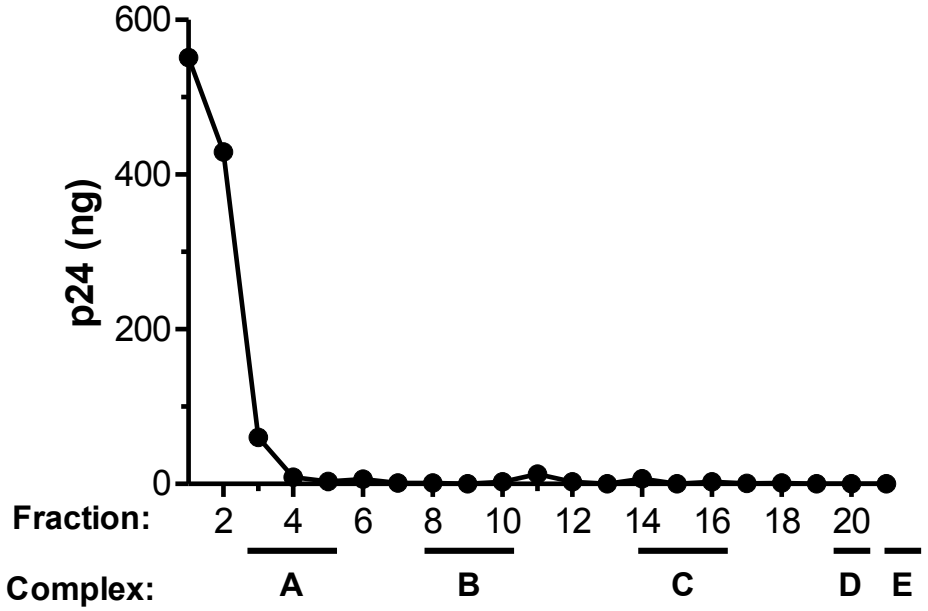

Figure 11. Distribution of CA in 5-45%/1 hr gradients. Levels of p24 from each fraction were determined by antigen ELISA. Fractions listed below graph; Complexes indicated below fractions. Data is representative of at least three independent experiments.

Given the aforementioned reports this result suggested that CA likely dissociated from both RTCs and PICs during the purification procedure.

Matrix (MA) sediments with vDNA complexes in VGC.

There is conflicting evidence for association of (MA) with RTCs and PICs. Fassati and Goff (2001) suggested that MA is not associated with RTCs. Bukrinsky et al. (1993) suggested MA was found in the same fractions as viral nucleic acids, and later, Miller, Farnet, and Bushman (1997) found MA sedimented with integration activity. To determine if MA remained associated with PICs purified by VGC, we detected the presence of MA in each fraction. To do this we infected cells with virus containing biotinylated MA as described in Belshan et al. (2009). This allowed for efficient capture of MA protein from each fraction. MA was affinity purified using streptavidin conjugated to agarose beads, separated by SDS-PAGE, and detected by Western blot with streptavadin-HRP (Figure 12, experiment performed by Dr. Michael Belshan). MA was detected in fractions 1 – 2, 7 – 15, and 20, corresponding to Complexes B, C and D. Complexes A and E did not contain detectable MA. The detection of MA in several fractions that contain integration activity (8 – 10 and 14 – 15) suggests that MA was associated with PICs purified by VGC.

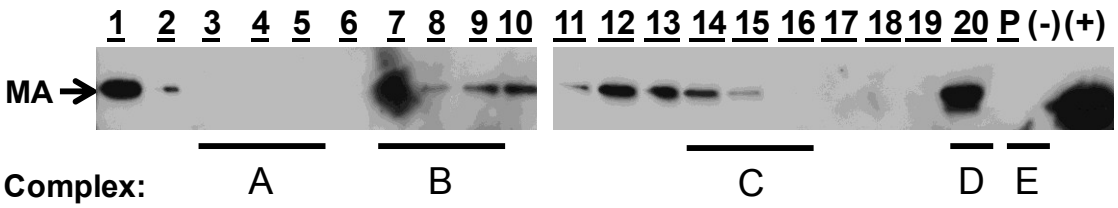

Figure 12. Distribution of MA in 5-45%/1 hr gradients. Anti-MA Western Blot analysis of affinity purified fractions using biotinylated MA. Fraction number is indicated (1= top of gradient). (-), Uninfected lysate; (+), purified virus particles (not tagged with biotin acceptor sequence), Complexes indicated below blot. Representative of two independent experiments.

The nucleoprotein complexes detected in gradients were not derived from viral particles.

To discount the possibility the Complexes identified in gradients were derived from viral particle contamination we characterized the sedimentation of DNase-treated virions with the same methods used to harvest and purify the NPCs. The profiles of the viral factors derived from purified virus particles are shown in Figure 13. Only background levels of vDNA were detected, indicating that the vDNA Complexes and PICs detected in gradients were not derived from contamination. Compared to sedimentation of vRNA in fractions 3 – 5, the majority of vRNA from virus particles sedimented to the bottom of the gradient (Figures 13A). The majority of RT activity remained soluble in the top three fractions of the gradient (Figure 13B) compared to the sedimentation of RTCs to fractions 3 – 7. Notably, the RT activity was dissociated from the vRNA in these gradients. Consistent with our overall findings, almost all virus particle-derived CA was detected in the top of the gradient, consistent with its dissociation with mild detergent (Figure 13C). The absence of vDNA and the differential sedimentation of vRNA and RT activity demonstrate that the PICs and RTCs purified by VGC are not derived from viral particle contamination.

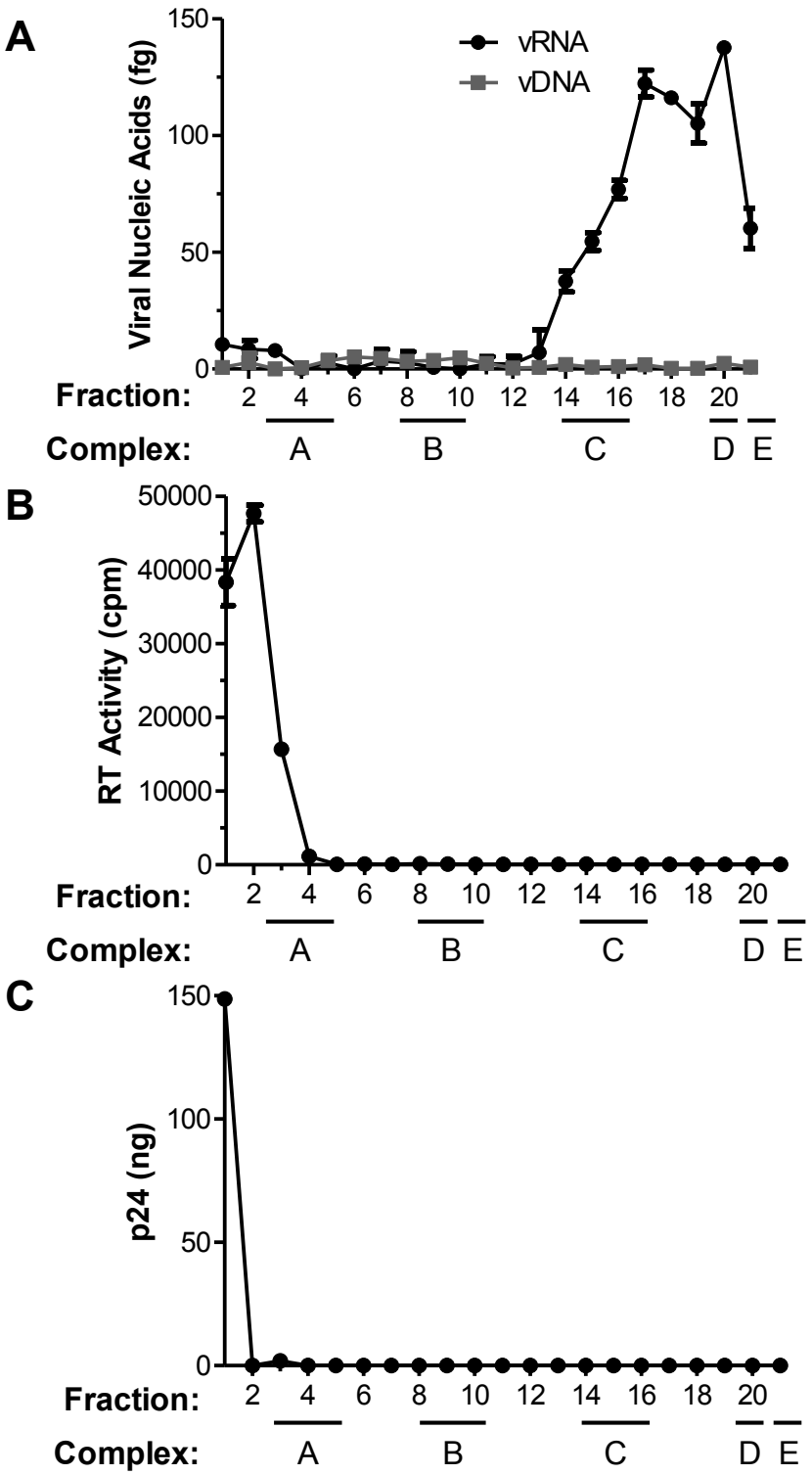

Figure 13. 1 hr gradients of lysed DNased-treated virus. **A.** vRNA and vDNA were extracted from each fraction and levels determined by quantitative real-time RT-PCR and quantitative real-time PCR. **B.** RT activity was determined by enzymatic incorporation. **C.** CA levels in each fraction were determined by antigen ELISA. Fractions listed below graph; Complexes indicated below fractions. Data is representative of three independent experiments, error bars represent standard deviation from triplicate real-time PCRs.

Chapter 2A:

Biophysical effects of prolonged ultracentrifugation on HIV-1 nucleoprotein complexes.

As part of our effort to purify HIV-1 NPCs and understand the biophysical properties of these complexes, we analyzed the sedimentation of viral NPCs 1) partially purified by extended ultracentrifugation (4 hr) that were produced by 2) 4 hr and 3) O/N infections. These findings demonstrate the labile nature of the HIV-1 NPCs and longer ultracentrifugation results in the disassociation of complexes. Moreover, the distribution of complexes in longer ultracentrifugation lengths supports our assertion that 5-45%/1 hr gradients are an advantageous method to purify HIV-1 NPCs.

Extended ultracentrifugation alters the pattern of vDNA distribution.

To determine the effect of extended ultracentrifugation time, we examined the distribution of vDNA from 4 hr infections in gradients centrifuged for 4 hr (4 hpi- 5-45%/4 hr). As with 5-45%/1 hr gradients, vDNA was detectable in all fractions of the 4 hpi- 5-45%/4 hr gradients. Distinct peaks were observed, however the pattern of vDNA sedimentation was markedly different compared to the 5-45%/1 hr gradients (Figure 14, gray line). The 4 hpi- 5-45%/4 hr (Figure 14, black line) gradients produced 4 complexes, labeled F – I from the top of the gradient. Surprisingly, the majority of the vDNA was in Complex F (fractions 5 – 9), the lowest molecular weight complex. This contrasts the 5-45%/1 hr gradients in which the majority of vDNA sedimented to fractions 14 – 16. Compared to Complex F, only small levels of vDNA were detected in fractions

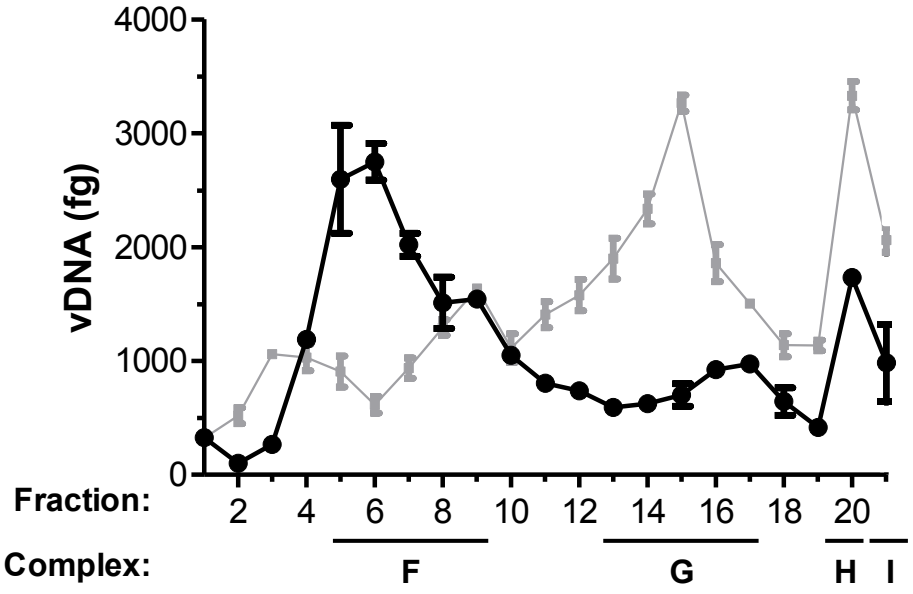

Figure 14. Distribution of vDNA in 4 hpi- 5-45%/4 hr gradients. vDNA was isolated from each fraction using a PCR purification kit and the levels determined by quantitative real-time PCR using HIV *gag*-specific primers. Black circles, vDNA from 4 hpi-5-45%/4 hr gradient; gray circles, vDNA from 5-45%/1 hr gradients; Fractions listed below gragh; Complexes indicated below fractions. Data is representative of at least 10 independent experiments, error bars indicate standard deviation from samples assayed by real-time PCR in triplicate.

14-16, the location of PICs in 5-45%/1 hr gradients. High levels of vDNA were detected in fraction 20 and the pellet, which was also observed in 5-45%/1 hr gradients.

Integration activity does not coincide with fractions containing the majority of vDNA in 4 hpi- 5-45%/4 hr gradients.

Next we determined which of the four vDNA Complexes contained integration activity in the 4 hpi- 5-45%/4 hr gradients. The average specific integration activities shown in Figure 15 represent the fractions of each Complex from a minimum of three independent experiments. Surprisingly, specific integration activity was detected only in fractions corresponding to Complexes G and H (Figure 15). Moreover, no integration activity was detected in the Complex containing the majority of vDNA (Complex F) or the remaining Complex, I. This result suggests the increased centrifugation time may cause dissociation of the PICs during centrifugation.

Reverse transcription complexes co-sediment with preintegration complexes in 4 hpi- 5-45%/4 hr gradients.

An important feature of 5-45%/1 hr gradients was the ability to separate RTCs from PICs. Given the markedly different results for PIC distribution from the 5-45%/1 hr gradients from the 4 hpi- 5-45%/4 hr gradients, we next determined the location of RTCs by measuring vRNA, RT activity, and ERT-vDNA levels in the fractions of 4 hpi- 5-45%/4 hr gradients (Figure 16). In contrast to the distribution pattern of vRNA in 5-45%/1 hr gradients, the majority of vRNA sedimented to the bottom of 4 hpi- 5-45%/4 hr gradients, starting with fraction 15 (Figure 16A). Similar to the co-sedimentation of vRNA with RT

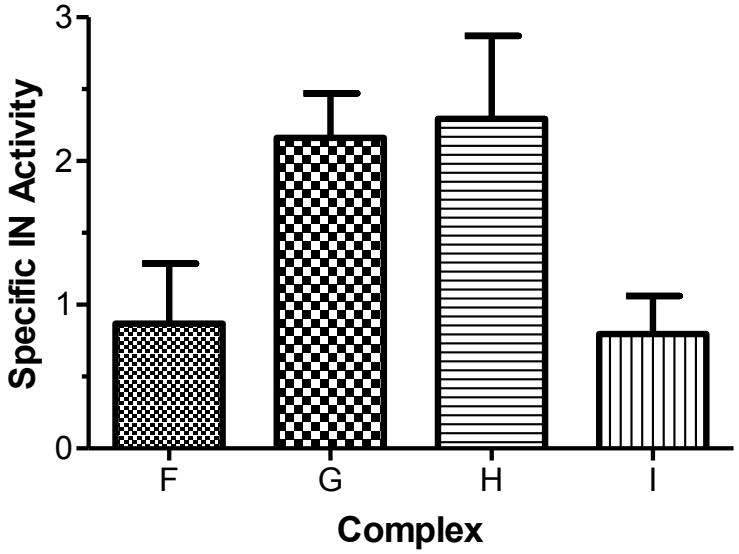

Figure 15. Integration activity of complexes in 4 hpi- 5-45%/4 hr gradients. Specific integration activity determined by calculating the specific integration of positive to negative samples from DNA levels. Complex F, G, H, and I = peak fractions from 4 hr gradients. Error bars indicate standard deviation from at least five independent experiments.

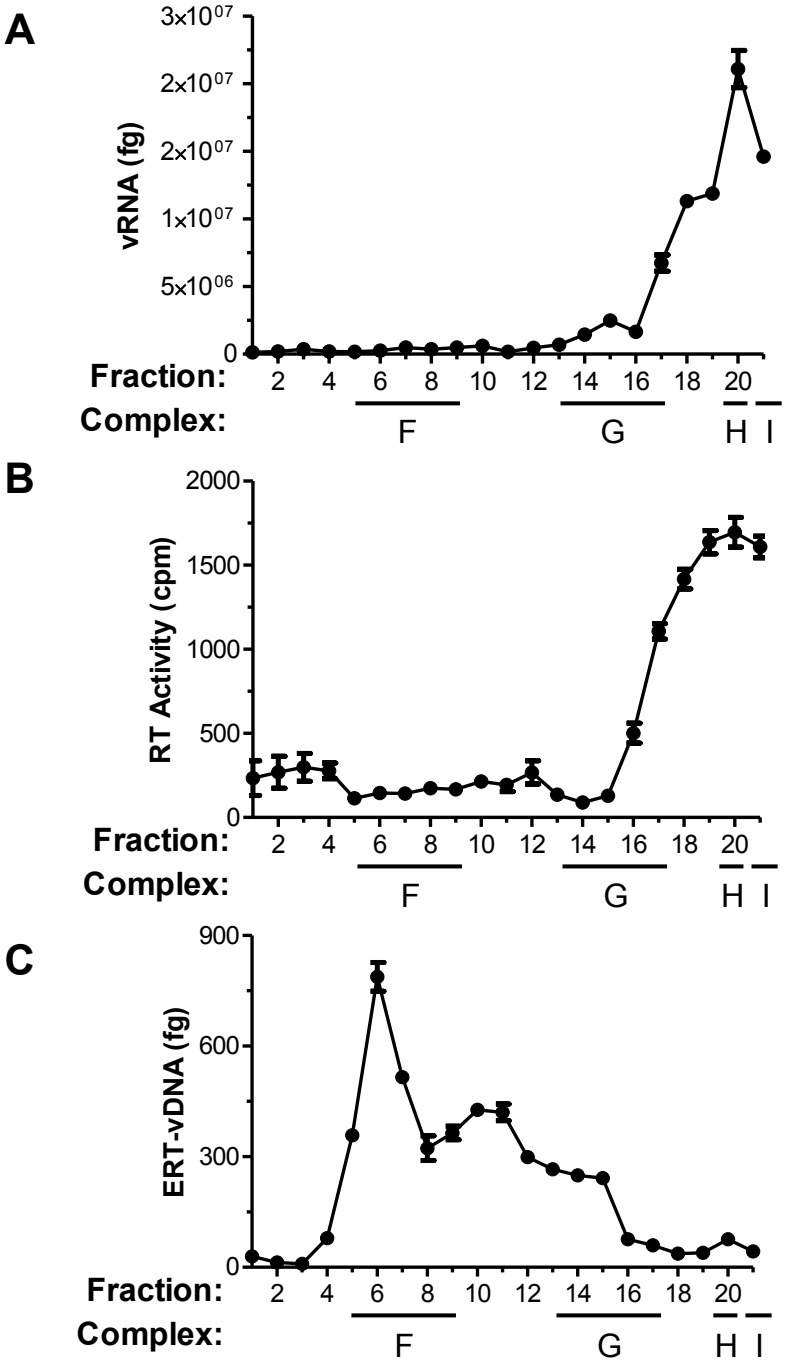

Figure 16. Distribution of RTC components in 4 hpi- 5-45%/4 hr gradients. **A.** vRNA was isolated from each fraction using a viral RNA extraction kit. RNA was treated with Turbo DNA-*free* and the levels determined by quantitative real-time RT-PCR using *gag*-specific primers. **B.** The RT activity present in fractions was determined by in vitro [32P]TTP-incorporation assay. **C.** ERT-vDNA was measured by quantitative real-time PCR using ERT-vDNA primers. Fractions listed below graph; Complexes indicated below fractions. Data is representative of at least three independent experiments, error bars indicate standard deviation from triplicate real-time PCRs.

activity in 5-45%/1 hr gradients, both co-sedimented in 4 hpi- 5-45%/4 hr, however this time in the bottom fractions of gradients (Figure 16B). The results of the 5-45%/1 hr and the 4 hpi- 5-45%/4 hr gradients suggest that the RTCs exhibit a constant sedimentation from 1 – 4 hrs. As explained above, the ERT-vDNA is distributed similarly to full-length vDNA, but higher concentrations were observed in Complex G (compare Figure 16C to Figure 14) but not in peak RTC fractions 18 – pellet. However some ERT-vDNA was observed to be associated with the PIC or RTC containing fractions. This contrasts the 5-45%/1 hr gradients where high levels of ERT-vDNA co-sedimented with both the vRNA and RT activity (3 – 6 for vRNA, 3 – 9 for RT activity, and 2 – 10 for ERT-vDNA). This may suggest that the extended centrifugation caused some dissociation of the RTCs. Despite this dissociation, the overlap of vRNA and RT activity with fractions containing integration activity indicates that the RTCs and PICs co-sedimented by 4 hr of centrifugation and suggests that the NPCs may be reaching equilibrium in the gradient.

Capsid remains in the top fractions of 4 hpi- 5-45%/4 hr gradients.

CA disassociated from NPCs and virus particles purified using 5-45%/1 hr gradients, therefore we expected similar results using 4 hpi- 5-45%/4 hr gradients. Indeed, CA was detected in the top of the gradient and did not migrate past fraction 5 (Figure 17). This was consistent with the dissociation of CA from NPCs extracted with mild detergent.

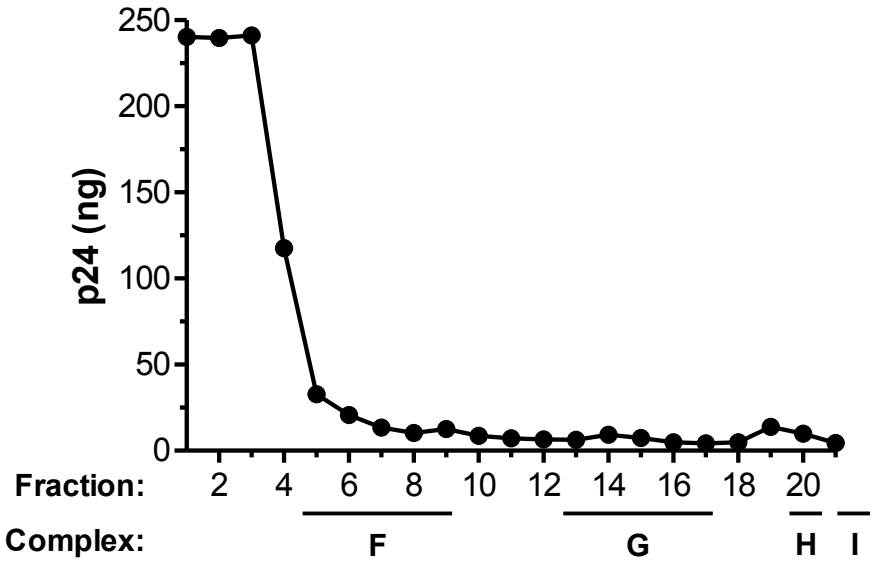

Figure 17. Distribution of CA in 4 hpi- 5-45%/4 hr gradients. Levels of p24 from each fraction were determined by antigen ELISA. Fractions listed below graph; Complexes indicated below fractions. Data is representative of three independent experiments.

Matrix distributes throughout all fractions in 4 hpi- 5-45%/4 hr gradients.

Next, we examined the sedimentation of MA in 4 hpi- 5-45%/4 hr gradients. MA was detected by Western blot of concentrated gradient fractions. This was a preliminary experiment. MA was observed in all fractions of the gradient; however the majority of MA was detected in the top fractions of the gradient (Figure 18; performed by Cameron Schweitzer). Only small levels of MA were detected in the fractions containing PICs and RTCs. This data suggests that increased length of centrifugation resulted in the diffusion of MA throughout the gradient and may provide evidence that an increased length of centrifugation diffuses complexes rather than concentrating them.

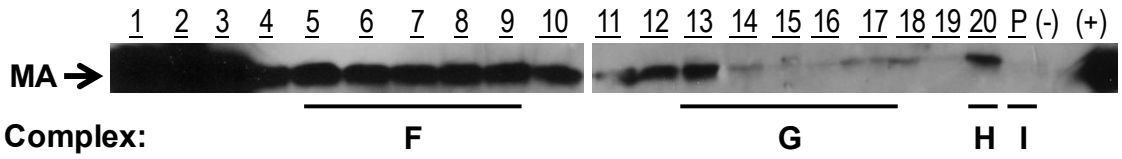

Figure 18. Distribution of MA in 4 hpi- 5-45% 4 hr gradients. A sample of each fraction was separated by SGS-PAGE and Western blotted for MA from HIV+VSVg infected lysates (Cameron Schweitzer). Fractions are listed above the lane; (-) = uninfected cells; (+) = concentrated virus; Complexes indicated below the blot. Data is from an individual, preliminary experiment.

Chapter 2B.

Biophysical effects of prolonged ultracentrifugation on HIV-1 nucleoprotein complexes from overnight infections.

Extended centrifugation of O/N infections alters vDNA distribution compared to shorter centrifugation and infection methods.

As an extension of our studies, we examined the distribution of NPCs from O/N infections purified by 4 hr gradient centrifugation (5-45%/4 hr). Again, the detection of vDNA was used to determine the distribution of Complexes in 5-45%/4 hr gradients. All fractions contained vDNA; and, 4 Complexes were identified by vDNA distribution (Figure 19) labeled J - M from the top of the gradient. Fractions 7 – 16 consist of two broader peaks that were more diffuse than peaks from other gradients. The greatest concentration of vDNA was detected in fraction 20 and the pellet (complexes L and M). Complex J (fractions 7 – 10) contained more vDNA than Complex K (fractions 14 – 16), but both had lower concentrations than fraction 20 and the pellet.

Reverse transcription and vDNA complexes co-sediment in 5-45%/4 hr gradients.

Since RTCs were separable from vDNA complexes by 5-45%/1 hr gradients but not by 4 hpi- 5-45%/4 hr gradients we wanted to determine whether this was a result of the extended centrifugation or the difference in infection length. The sedimentation of RTCs was again determined by detecting the presence of vRNA, RT activity, and ERT-vDNA (Figure 20). vRNA was detectable in all fractions, but the majority distributed to the top of the gradient. vRNA peaked at fraction 4 and declined until fraction 16, with a

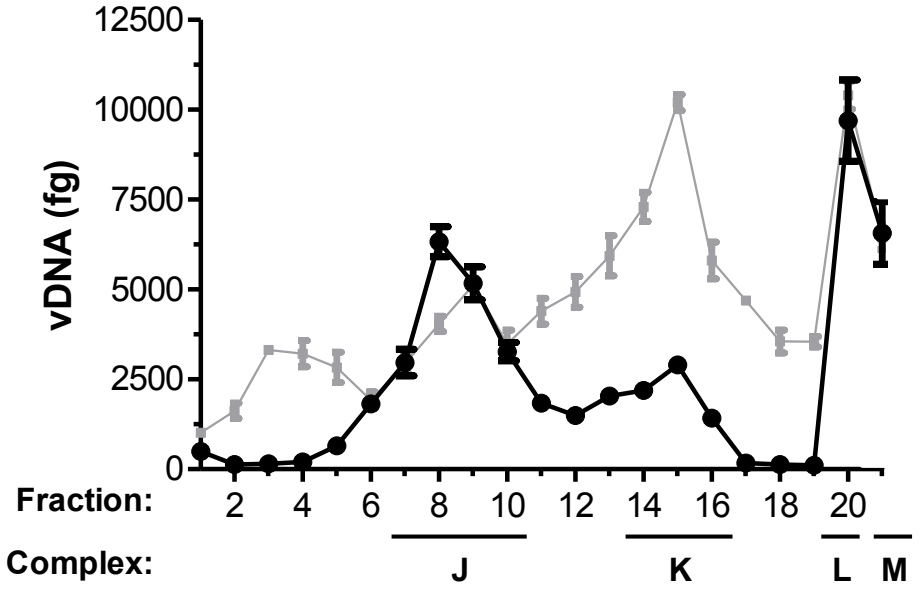

Figure 19. Distribution vDNA of 5-45%/4 hr gradietns. vDNA was isolated from each fraction using a PCR purification kit and the levels determined by quantitative real-time PCR using HIV *gag*-specific primers. Fractions listed below gragh; Complexes listed below fractions; black circles, vDNA from 5-45%/4 hr gradients; gray circles, vDNA from 5-45%/1 hr gradients. Data is representative of at least four independent experiments, error bars indicate standard deviation from real-time PCR samples assayed in triplicate.

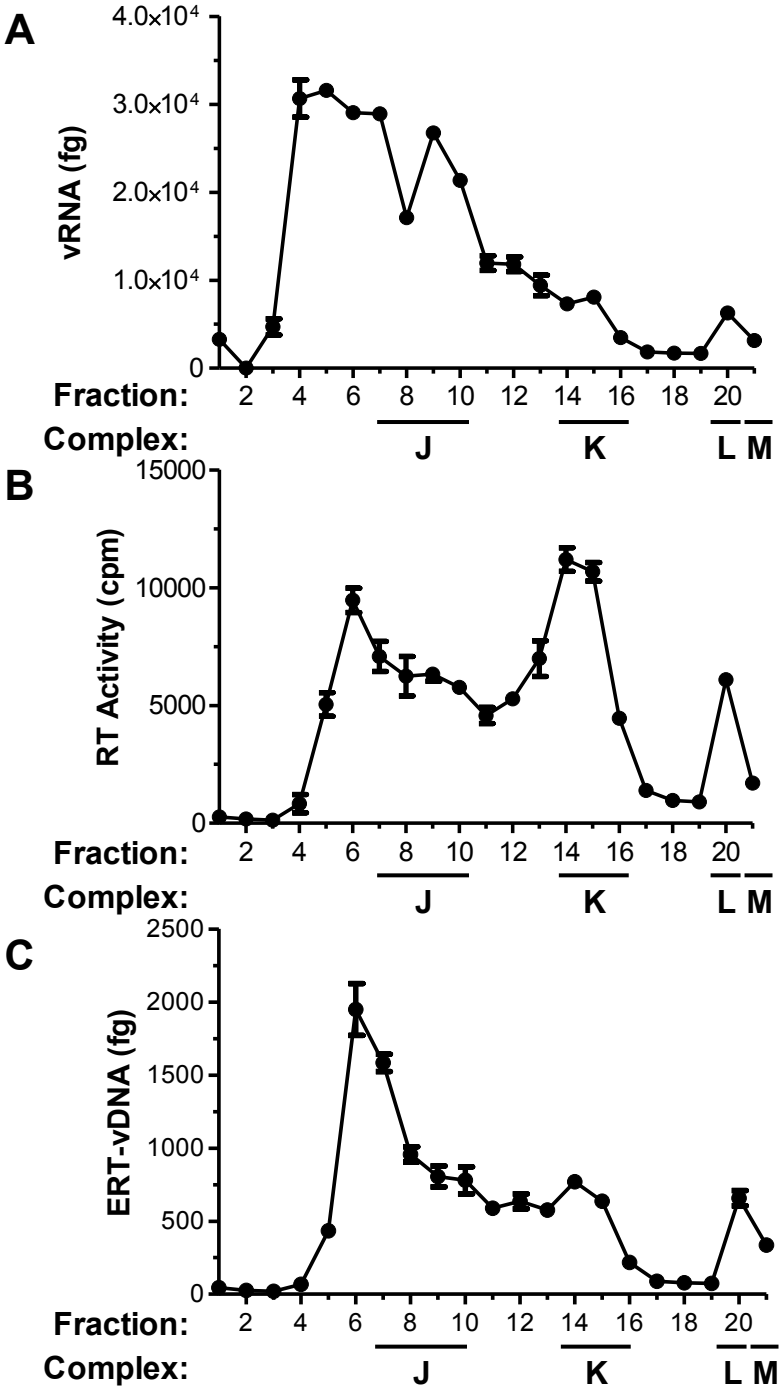

Figure 20. Distribution of RTC components in 5-45%/4 hr gradients. **A.** vRNA was isolated from each fraction using a viral RNA extraction kit. RNA was treated with Turbo DNA-*free* and the levels determined by quantitative real-time RT-PCR using *gag*-specific primers. **B.** The RT activity present in fractions was determined by in vitro [32P]TTP-incorporation assay. **C.** ERT-vDNA was measured by quantitative real-time PCR using ERT-vDNA primers. Fractions listed below graph; Complexes indicated below fractions. Data is representative patterns of at least three independent experiments, error bars indicate standard deviation from triplicate real-time PCRs.

small peak present in fraction 20 (Figure 20A). This was in sharp contrast to the 4 hpi-5-45%/4 hr gradients in which the vRNA sedimented to the bottom of the gradient. The peak of vRNA in the 5-45%/4 hr gradient centrifugation was similar, but broader than the sedimentation of vRNA in 5-45%/1 hr gradients. RT activity distributed in three peaks, the first two peaks (fraction 5 – 9 and 13 – 16) were not distinct from each other but overlapped the vRNA (Figure 20B). In each purification method the vRNA and RT activity sedimented with each other but to different locations in the gradients (compare Figures 10, 16, and 20). The ERT-vDNA exhibited a similar distribution to the full length vDNA; accordingly, the majority of ERT-vDNA detected in fractions 5 – 8, with a peak containing less ERT-vDNA in Fractions 13 – 15. Therefore, the ERT-vDNA distribution was similar among all the infection and VGC protocols. Consistent with our previous data, CA remained at the top of the 5-45%/4 hr gradient due to dissociation as a result of lysis of cells with detergent (Figure 21). In summary, the majority of vDNA, vRNA, RT activity, and ERT-vDNA were detected in the same fractions of 5-45%/4 hr gradients indicating that, the RTCs and vDNA co-sedimented. These results demonstrate that extended ultracentrifugation results in the dissociation of viral NPCs regardless of the infection method.

The nucleoprotein complexes detected in 4 hr gradients were not derived from viral particles.

Similar to the 1 hr centrifugation studies we performed a battery of assays on purified virus particles to confirm that the complexes identified in 4 hr gradients were not derived from viral particles. Again, the level of vDNA detected was 100-fold less than levels observed from purified HIV-1 NPCs. The only measurable amount of vRNA was

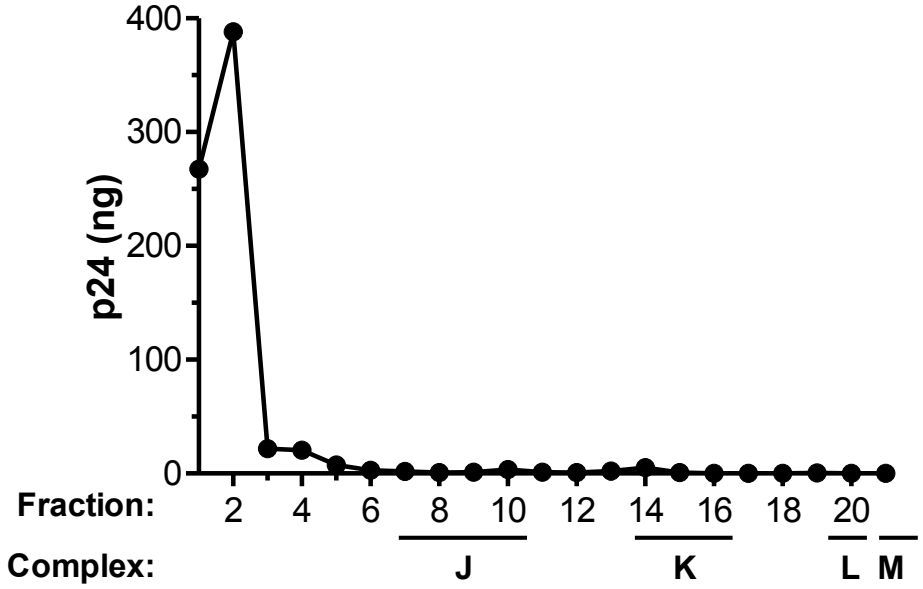

Figure 21. Distribution of CA in 5-45%/4 hr gradients. Levels of p24 from each fraction were determined by antigen ELISA. Fractions listed below graph; Complexes indicated below fractions. Data is representative of three independent experiments.

detected in fraction 20 and the pellet (Complex H and I; Figure 22A). The majority of RT activity was detected at the top of the gradient and did not overlap with any Complexes (Figure 22B). Consistent with all other assays, the majority of CA was detected at the top of the gradient which did not overlap with any Complexes (Figure 22C). The lack of vDNA, and the vRNA and RT activity distribution compared to the distribution of factors in the gradients of HIV-1 NPCs indicates that neither the PICs nor RTCs are derived from viral particles contaminants.

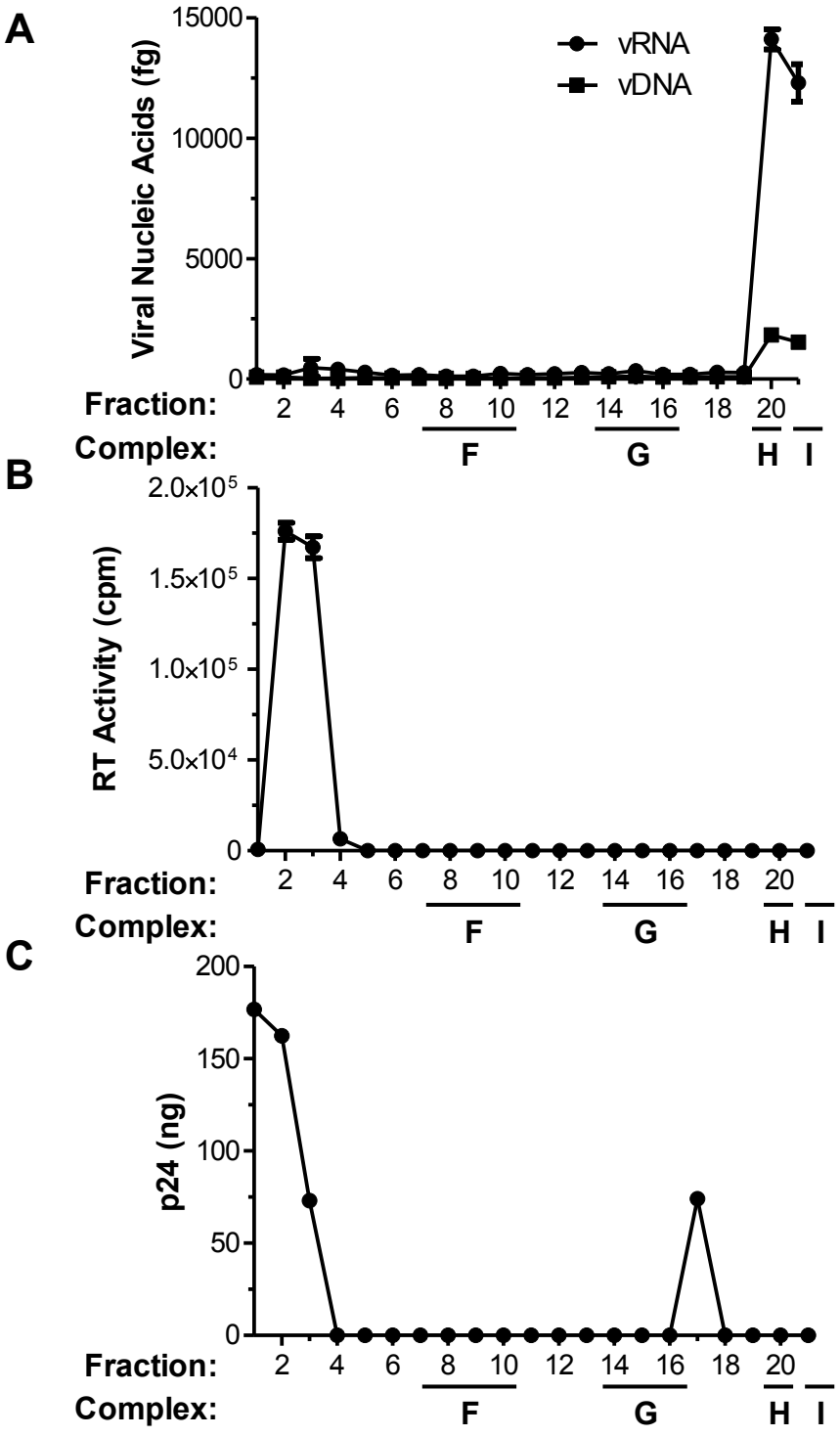

Figure 22 4 hr gradients of lysed, Dnase-treated virus. **A.** vRNA and vDNA were extracted from each fraction and levels determined by quantitative real-time RT-PCR and quantitative real-time PCR. **B.** RT activity was determined by enzymatic incorporation. **C.** CA levels in each fraction were determined by antigen ELISA. Fractions listed below graph; Complexes indicated below fractions. Data is representative at least three independent experiments. Error bars indicate standard deviation from real=time PCR samples assayed in triplicate.

DISCUSSION

The nucleoprotein complexes (NPCs) present during the early steps of HIV-1 infection are critical for the synthesis and targeting of the viral DNA to the host cell chromosomal DNA. The PIC is a unique viral structure and as such is a potential target for the development of inhibitors. However, no antiretroviral compounds targeting the PIC are in development due to the lack of understanding of its structure. The prospect for the development of inhibitors targeting PICs remains discouraging until improvements in the purification processes of these complexes leads to additional biochemical analyses of the structure and function of the NPCs. The lability of retroviral NPCs has made biochemical and proteomic studies of these complexes challenging. The long-term goal of the lab is to ascertain the viral proteins present in the complexes as well as identifying cellular proteins that are required for RTC and PIC transport and function. The first critical step toward understanding PIC structure is to purify biologically active complexes.

In these studies we investigated methods to purify PICs utilizing velocity gradient centrifugation (VGC). Only one other report has detected integration activity in gradient fractions (Farnet and Haseltine 1990) therefore we set out to determine biophysical properties of integration competent complexes. In these studies I demonstrated the purification of PICs by 1 hr VGC through 5-45% sucrose (w/v) gradients at 41,000 rpm (207,000 x*g* average) into fractions 14 – 16. This was shown by the co-sedimentation of previously described PIC-associated viral factors: peak levels of vDNA and integration activity, the MA protein, and low levels of vRNA and RT activity. Importantly, I concluded that complexes identified in 5-45%/1 hr gradients were not due to

contaminating viral particles. This was shown by the VGC control experiments using virus particles in which there was an absence of vDNA and differential sedimentation patters of vDNA, vRNA and RT activity.

In addition to purifying active PICs, the 5-45%/1 hr gradient protocol was able to separate them from RTCs, a previously unpublished observation. This was shown by the presence of vRNA, RT activity, and ERT-vDNA in top half of the gradient (fractions 2 – 10), and the highest levels of vDNA and integration activity in fractions 14 – 16. The sedimentation rate of the complexes suggests that the RTCs are smaller in size than PICs, although would be necessary to determine the S values for these complexes.

Overnight infection of C8166-45 cells by spinoculation is the optimal method to produce HIV-1 preintegration complexes.

The literature contains diverse and inconsistent infection and purification methods for isolating PICs. For example numerous cells lines, infection length, virus clones, and lysis methods have been used. Given the diversity of previous methods used, our first objective was to define the most efficient technique to produce PICs. We explored several parameters, including cell type, virus clone, infection method, and the length of infection. Among all the parameters we tested, spinoculation coupled with the O/N infection of C8166-45 cells produced the highest levels of infection and recoverable levels of PIC activity. The levels of vDNA and the amount of integration activity detected in O/N infections were 10-fold higher than the levels detected for 4 hr and 6 hr infections. These results were surprising because several previous studies suggest that the peak level of infection occurs at earlier time points. Farnet and Haseltine (1990) observed that the maximum levels of vDNA were detected 6 hr post infection and virtually no

vDNA was detectable by 15 hr post infection in SupT1 cells; and Heinzinger et al. (1994) detected no increase in vDNA from 5 hr to 48 hr post infection. Somewhat unexpectedly, RTCs were also detected in O/N infections. This contrasts with Fassati and Goff's (2001) observation that RTCs were not detectable in HeLa cells past 7 hr post infection. However, a similar effect of spinoculation was observed (an 11-fold increase in spinoculated infections compared to non-spinoculated) as O'Doherty, Swiggard, and Malim (2000), who observed a 40-fold increase in vDNA levels in 5 hr post infection in CEM-SS cells. We also tested co-culture infections which have been reported to produce high levels of infection and PIC activity (Bukrinskaya et al. 1998; Brown et al. 1987). Although we observed high levels of infection in both acute and co-culture infections, the levels obtained from either method were less than those obtained with the O/N C8166-45 cell infection protocol. Furthermore, we find the co-culture method of infection disadvantageous since the infections are non-synchronous, which likely results in a mixture of NPCs representing various stages of the early viral life cycle at the time of harvest.

Improvement of the *in vitro* integration assay.

As part of these studies we improved a previously published $_{Q}$PCR-based in vitro integration assay (Engelman 2009) that we also used in a related study in our laboratory to test the functionality of an IN clone with an inserted tag (Belshan et al. 2009). The original nested PCR assay utilized dilutions of a wild-type PIC sample to generate a standard curve. Thus the integration activity of all variable samples were measured as a percentage of the wild-type samples. Since the activity of any given sample varies from experiment to experiment, this approach is limited because a new standard curve must

be generated for each experiment. To overcome these restrictions, we constructed a plasmid DNA standard for the nested $_{Q}$PCR assay. The use of this standard allows for inter-experiment comparisons of integration activity. It should be noted however that since the LTR is in a fixed position in the standard plasmid (whereas the integration events are random within the target plasmid) the data obtained from the assay is a relative quantification and does not represent the exact number of integration events.

Velocity gradient centrifugation as a method to purify HIV-1 preintegration complexes.

Both density and velocity gradients have been used to purify HIV-1 NPCs. A variety of sucrose gradients and centrifugation parameters have been used including: 5 – 20% at 50,000 x *g* for 1 hr followed by 20 – 70% at 117,000 x *g* for 20 hr (Fassati and Goff 2001), 15 – 30% at 150,000 x *g* for 3 hr (Bukrinsky et al. 1993; Farnet and Haseltine 1990; Farnet and Haseltine 1991), and 10 – 50% at 155,000 x *g* for 2 hr (Miller, Farnet, and Bushman 1997). Not surprisingly, these studies produced a diversity of sedimentation patterns for viral factor. Another compounding factor that may contribute to the variable data is the methods used to fractionate gradients. To fractionate, these studies used either a Densi-Flow apparatus (Bukrinsky et al. 1993; Miller, Farnet, and Bushman 1997) or collected fractions by puncturing a hole in the bottom of the gradient (Fassati and Goff 2001; Farnet and Haseltine 1990; Farnet and Haseltine 1991). Both methods of fractionation result in a large amount of fraction mixing. To overcome these problems I formed and fractionated gradients using the BioComps' Gradient Station. This apparatus mixes six identical gradients at a time and retrieves uniform fractions. Moreover, in contrast to the other methods of fractionation,

the Gradient Station Fractionator washes the collection line between fractions, practically eliminating fraction mixing. There features combine to allow us to concentrate near exact fractions from replicate gradients, allowing the comparison of the sedimentation of factors from gradients in different experiments.

During our studies we examined many gradient parameters. Most notably, when the time was increased there were changes in the sedimentation of all viral factors, except CA. This was evident by the strikingly different vDNA profiles between the 1 hr and 4 hr centrifugation lengths. In 5-45%/1 hr gradients the vDNA distributed into 5 vDNA Complexes, the peak complex (14 – 16) that contained the greatest concentration of vDNA also possessed the highest levels of integration activity. In contrast, the NPCs purified by 4 hpi- 5-45%/4 hr gradients distributed in 4 vDNA Complexes and the largest peak (fractions 5 – 9) did not contain integration activity. Instead, the greatest amount of integration activity was detected in fraction 20 which did not contain the majority of vDNA. Some integration activity was present in fractions 13 – 17, but contained only low levels of vDNA. Moreover, the MA protein diffused throughout the 4 hr gradients instead of co-sedimenting with some of the PICs. The different sedimentation profile of the majority of the vDNA and MA from the integration activity suggested that the increased centrifugation length results in disassociation of the PIC.

Surprisingly, the distribution profiles of the viral components were also different in the 5-45%/4 hr gradients (O/N infection) compared to the 4 hpi- 5-45%/4 hr gradient. Specifically, the amount of vDNA in the first two peaks (fractions 7 – 10 and 14 – 16) were similar in size in the 5-45%/4 hr gradients, whereas the first peak (fractions 5 – 9) of vDNA was consistently larger in the 4 hpi- 5-45%/4 hr gradients. This suggests that the higher density of complexes in the O/N infections leads to a perceived decrease in complex dissociation during 4 hr VGC. We suspect that this was due to a higher density

of complexes in the O/N infections compared to the 4 hr infections as shown by the time-course data. Alternatively, the complexes present in O/N infections may be more stable than those from 4 hr infections.

One interesting phenomenon we observed was that, integration activity was detected in Fractions 14 – 16 despite the differences in peak levels of vDNA in both 1 hr and 4 hr gradients. This provides evidence that fractions 14 – 16 contain a density of sucrose that specifically retards PIC sedimentation. To confirm these data, future studies should assay the sedimentation of PICs produced from O/N infections in the 5-45%/4 hr gradients. We hypothesize that due to the increase concentration of complexes, more PIC activity will be observed in fraction 14 – 16 compared to that detected in 4 hpi- 5-45%/4 hr gradients; however, integration activity will still be observed in fraction 20 due to extended sedimentation of the complexes during the increased centrifugation.

Increased centrifugation length has deleterious affects on HIV-1 preintegration complexes.

Independent of infection length, an increase of ultracentrifugation time to 4 hr resulted in the co-sedimentation of RTCs and PICs which suggests that both complexes reach their density equilibrium rapidly. Based on the aforementioned data we conclude that the longer length of centrifugation is not ideal for purifying PICs from RTCs for biochemical analyses. Most previous reports used 2 hr or 4 hr gradients, and do not report the extent to which they examined different centrifugation times (Fassati and Goff 2001; Bukrinsky et al. 1993; Farnet and Haseltine 1990; Miller, Farnet, and Bushman 1997; Farnet and Haseltine 1991). Since most of these studies did not assay PIC

activity it is not clear whether they observed a separation of RTCs and PICs. Our data would suggest that they likely concentrated both RTCs and PICs and detected factors from both complexes (Fassati and Goff 2001; Bukrinsky et al. 1993; Farnet and Haseltine 1991). Our studies clearly show that a shorter centrifugation length is ideal for purifying PICs. However, our studies did not examine another factor contributing the force on the complexes – the speed of centrifugation. Given that the total force exerted on the complexes is a function of both speed and time and our observation that increased time dissociated PICs, we hypothesize that reducing the speed may also enhance the recovery of PICs.

As expected, capsid did not co-sediment with HIV-1 nucleoprotein complexes.

A number of recent studies have focused on the necessity of a proper rate of CA uncoating after the virus entry to facilitate efficient completion of the early steps of HIV-1 replication. One study described a CA mutation that resulted in viruses that were able to undergo reverse transcription but were unable to import into the nucleus (Dismuke and Aiken 2006). Current data suggests that CA is not associated with PICs and possibly loosely associated with RTCs (Fassati and Goff 2001; Bukrinsky et al. 1993; Farnet and Haseltine 1990; Miller, Farnet, and Bushman 1997; Farnet and Haseltine 1991). We observed the majority of CA at the top of all gradients. This region contains the majority of the soluble cellular proteins and did not contain any HIV-1 NPCs, consistent with the dissociation and solubilization of CA from the HIV-1 core and NPCs. This trend has been previously observed by several groups utilizing hypotonic lysis (Fassati and Goff 2001; Bukrinsky et al. 1993), mild detergent lysis (Farnet and Haseltine 1990; Miller, Farnet, and Bushman 1997; Farnet and Haseltine 1991) and cells infected by co-culture that

were lysed with mild detergent (Karageorgos, Li, and Burrell 1993). Thus, our protocol may not be useful for studying the role of CA in HIV-1 NPC structure/function.

Variability in the bottom of gradients is likely due to contamination from gradient fractions.

Fractionating with the Biocomp Gradient Station produces more uniform fractions than the other methods discussed above. However when the piston enters the gradient and as it collects the fractions down the gradient some leakage through the seal occurs. Any leakage that occurs during the fraction collection is released into fraction 20 as the piston retracts from the gradient tube. For this reason, fraction 20 contains variable amounts of components from other fractions. Furthermore, fraction 20 is removed from the gradient tube manually which likely disturbs the pellet during aspiration. Due to these side-effects of fractionation, in most of the gradients, fraction 20 and the pellet are contaminated with other fractions. Indeed, we observed higher levels of error in the measurements of viral factors in fraction 20 and the pellet. The amount of leakage varied from gradient to gradient and thus so did the observed amount of viral factors in fraction 20 and the pellet. This supports our assertion that the 5-45%/4 hr VGC protocol is not idea for purifying HIV-1 NPCs. That withstanding, the unique presence of a viral factor in fraction 20 alone, such as the integration activity observed in 4 hpi- 5-45%/4 hr gradients, indicates the bona fide presence of that factor in that fraction. We recommend that future studies utilize centrifugation parameters that do not sediment complexes to fraction 20 and the bottom of the tube to avoid the ill effects of fraction contamination.

In summary, this study describes an optimal infection protocol and a method to purify NPCs. In comparison to previous methods, this protocol now allows us to purify complexes in a uniform manner. The effectiveness of our 1 hr gradients in separating RTCs and PICs suggests that these parameters are optimal for purifying active PICs, whereas previously published methods likely resulted in the co-sedimentation of the RTCs and PICs (Fassati and Goff 2001; Bukrinsky et al. 1993). These partially purified complexes can then be subjected to proteomic analyses to identify new cellular factors associated with PICs. These identified interacting cellular proteins can then be assessed for their role and/or requirement in viral replication. Identified interacting cellular proteins will hopefully yield new targets for the development of antiretroviral therapies.

References

Adamson, C. S., and E. O. Freed. 2008. Recent progress in antiretrovirals--lessons from resistance. *Drug Discovery Today* 13, (9-10) (May): 424-32.

Arfi, V., J. Lienard, X. N. Nguyen, G. Berger, D. Rigal, J. L. Darlix, and A. Cimarelli. 2009. Characterization of the behavior of functional viral genomes during the early steps of human immunodeficiency virus type 1 infection. *Journal of Virology* 83, (15) (Aug): 7524-35.

Arhel, N., A. Genovesio, K. A. Kim, S. Miko, E. Perret, J. C. Olivo-Marin, S. Shorte, and P. Charneau. 2006. Quantitative four-dimensional tracking of cytoplasmic and nuclear HIV-1 complexes. *Nature Methods* 3, (10) (Oct): 817-24.

Arhel, N. J., S. Souquere-Besse, S. Munier, P. Souque, S. Guadagnini, S. Rutherford, M. C. Prevost, T. D. Allen, and P. Charneau. 2007. HIV-1 DNA flap formation promotes uncoating of the pre-integration complex at the nuclear pore. *The EMBO Journal* 26, (12) (Jun 20): 3025-37.

Armon-Omer, A., A. Graessmann, and A. Loyter. 2004. A synthetic peptide bearing the HIV-1 integrase 161-173 amino acid residues mediates active nuclear import and binding to importin alpha: Characterization of a functional nuclear localization signal. *Journal of Molecular Biology* 336, (5) (Mar 5): 1117-28.

Belshan, M., C. J. Schweitzer, M. R. Donnellan, R. Lu, and A. Engelman. 2009. In vivo biotinylation and capture of HIV-1 matrix and integrase proteins. *Journal of Virological Methods* 159, (2) (Aug): 178-84.

Bowerman, B., P. O. Brown, J. M. Bishop, and H. E. Varmus. 1989. A nucleoprotein complex mediates the integration of retroviral DNA. *Genes & Development* 3, (4) (Apr): 469-78.

Brown, H. E., H. Chen, and A. Engelman. 1999. Structure-based mutagenesis of the human immunodeficiency virus type 1 DNA attachment site: Effects on integration and cDNA synthesis. *Journal of Virology* 73, (11) (Nov): 9011-20.

Brown, P. O., B. Bowerman, H. E. Varmus, and J. M. Bishop. 1987. Correct integration of retroviral DNA in vitro. *Cell* 49, (3) (May 8): 347-56.

Bukrinskaya, A., B. Brichacek, A. Mann, and M. Stevenson. 1998. Establishment of a functional human immunodeficiency virus type 1 (HIV-1) reverse transcription complex involves the cytoskeleton. *The Journal of Experimental Medicine* 188, (11) (Dec 7): 2113-25.

Bukrinsky, M. I., N. Sharova, M. P. Dempsey, T. L. Stanwick, A. G. Bukrinskaya, S. Haggerty, and M. Stevenson. 1992. Active nuclear import of human immunodeficiency virus type 1 preintegration complexes. *Proceedings of the National Academy of Sciences of the United States of America* 89, (14) (Jul 15): 6580-4.

Bukrinsky, M. I., N. Sharova, T. L. McDonald, T. Pushkarskaya, W. G. Tarpley, and M. Stevenson. 1993. Association of integrase, matrix, and reverse transcriptase antigens of human immunodeficiency virus type 1 with viral nucleic acids following acute infection. *Proceedings of the National Academy of Sciences of the United States of America* 90, (13) (Jul 1): 6125-9.

Christ, F., W. Thys, J. De Rijck, R. Gijsbers, A. Albanese, D. Arosio, S. Emiliani, et al. 2008. Transportin-SR2 imports HIV into the nucleus. *Current Biology : CB* 18, (16) (Aug 26): 1192-202.

Dismuke, D. J., and C. Aiken. 2006. Evidence for a functional link between uncoating of the human immunodeficiency virus type 1 core and nuclear import of the viral preintegration complex. *Journal of Virology* 80, (8) (Apr): 3712-20.

Ebina, H., J. Aoki, S. Hatta, T. Yoshida, and Y. Koyanagi. 2004. Role of Nup98 in nuclear entry of human immunodeficiency virus type 1 cDNA. *Microbes and Infection / Institut Pasteur* 6, (8) (Jul): 715-24.

Engelman, A. 2009. Isolation and analysis of HIV-1 preintegration complexes. *Methods in Molecular Biology (Clifton, N.J.)* 485, : 135-49.

Farnet, C. M., and W. A. Haseltine. 1991. Determination of viral proteins present in the human immunodeficiency virus type 1 preintegration complex. *Journal of Virology* 65, (4) (Apr): 1910-5.

Farnet, C. M., and W. A. Haseltine. 1990. Integration of human immunodeficiency virus type 1 DNA in vitro. *Proceedings of the National Academy of Sciences of the United States of America* 87, (11) (Jun): 4164-8.

Fassati, A., and S. P. Goff. 2001. Characterization of intracellular reverse transcription complexes of human immunodeficiency virus type 1. *Journal of Virology* 75, (8) (Apr): 3626-35.

Fassati, A., D. Gorlich, I. Harrison, L. Zaytseva, and J. M. Mingot. 2003. Nuclear import of HIV-1 intracellular reverse transcription complexes is mediated by importin 7. *The EMBO Journal* 22, (14) (Jul 15): 3675-85.

Gallay, P., V. Stitt, C. Mundy, M. Oettinger, and D. Trono. 1996. Role of the karyopherin pathway in human immunodeficiency virus type 1 nuclear import. *Journal of Virology* 70, (2) (Feb): 1027-32.

Gallay, P., S. Swingler, J. Song, F. Bushman, and D. Trono. 1995. HIV nuclear import is governed by the phosphotyrosine-mediated binding of matrix to the core domain of integrase. *Cell* 83, (4) (Nov 17): 569-76.

Goff, S., P. Traktman, and D. Baltimore. 1981. Isolation and properties of moloney murine leukemia virus mutants: Use of a rapid assay for release of virion reverse transcriptase. *Journal of Virology* 38, (1) (Apr): 239-48.

Greene, W. C., and B. M. Peterlin. 2002. Charting HIV's remarkable voyage through the cell: Basic science as a passport to future therapy. *Nature Medicine* 8, (7) (Jul): 673-80.

Heinzinger, N. K., M. I. Bukinsky, S. A. Haggerty, A. M. Ragland, V. Kewalramani, M. A. Lee, H. E. Gendelman, L. Ratner, M. Stevenson, and M. Emerman. 1994. The vpr protein of human immunodeficiency virus type 1 influences nuclear localization of viral nucleic acids in nondividing host cells. *Proceedings of the National Academy of Sciences of the United States of America* 91, (15) (Jul 19): 7311-5.

Karageorgos, L., P. Li, and C. Burrell. 1993. Characterization of HIV replication complexes early after cell-to-cell infection. *AIDS Research and Human Retroviruses* 9, (9) (Sep): 817-23.

Lapadat-Tapolsky, M., H. De Rocquigny, D. Van Gent, B. Roques, R. Plasterk, and J. L. Darlix. 1993. Interactions between HIV-1 nucleocapsid protein and viral DNA may have important functions in the viral life cycle. *Nucleic Acids Research* 21, (4) (Feb 25): 831-9.

Limon, A., N. Nakajima, R. Lu, H. Z. Ghory, and A. Engelman. 2002. Wild-type levels of nuclear localization and human immunodeficiency virus type 1 replication in the absence of the central DNA flap. *Journal of Virology* 76, (23) (Dec): 12078-86.

McDonald, D., M. A. Vodicka, G. Lucero, T. M. Svitkina, G. G. Borisy, M. Emerman, and T. J. Hope. 2002. Visualization of the intracellular behavior of HIV in living cells. *The Journal of Cell Biology* 159, (3) (Nov 11): 441-52.

Miller, M. D., C. M. Farnet, and F. D. Bushman. 1997. Human immunodeficiency virus type 1 preintegration complexes: Studies of organization and composition. *Journal of Virology* 71, (7) (Jul): 5382-90.

Mocroft, A., B. Ledergerber, J. P. Viard, S. Staszewski, M. Murphy, A. Chiesi, A. Horban, et al. 2004. Time to virological failure of 3 classes of antiretrovirals after initiation of highly active antiretroviral therapy: Results from the EuroSIDA study group. *The Journal of Infectious Diseases* 190, (11) (Dec 1): 1947-56.

Moore, M. S., and G. Blobel. 1992. The two steps of nuclear import, targeting to the nuclear envelope and translocation through the nuclear pore, require different cytosolic factors. *Cell* 69, (6) (Jun 12): 939-50.

Mougel, M., L. Houzet, and J. L. Darlix. 2009. When is it time for reverse transcription to start and go? *Retrovirology* 6, (Mar 4): 24.

O'Doherty, U., W. J. Swiggard, and M. H. Malim. 2000. Human immunodeficiency virus type 1 spinoculation enhances infection through virus binding. *Journal of Virology* 74, (21) (Nov): 10074-80.

Perno, C. F., G. Moyle, C. Tsoukas, W. Ratanasuwan, J. Gatell, and M. Schechter. 2008. Overcoming resistance to existing therapies in HIV-infected patients: The role of new antiretroviral drugs. *Journal of Medical Virology* 80, (4) (Apr): 565-76.

Poljak, L., S. M. Batson, D. Ficheux, B. P. Roques, J. L. Darlix, and E. Kas. 2003. Analysis of NCp7-dependent activation of HIV-1 cDNA integration and its conservation among retroviral nucleocapsid proteins. *Journal of Molecular Biology* 329, (3) (Jun 6): 411-21.

Sato, Hironori, Jan Orenstein, Dimiter Dimitrov, and Malcolm Martin. 1992. Cell-to-cell spread of HIV-1 occurs within minutes and may not involve the participation of virus particles. *Virology* 186, : 712-24.

Smith, S.D., M. Shatsky, P.S. Cohen, R. Warnke, M.P. Link, and B.E. Glader. 1984. Monoclonal antibody and enzymatic profiles of human malignant T-lymphoid cells and derived cell lines. *Cancer Research 44,* (12 Pt 1) (Dec): 5657-60.

Suzuki, Y., and R. Craigie. 2007. The road to chromatin - nuclear entry of retroviruses. *Nature Reviews.Microbiology* 5, (3) (Mar): 187-96.

Willey, R. L., D. H. Smith, L. A. Lasky, T. S. Theodore, P. L. Earl, B. Moss, D. J. Capon, and M. A. Martin. 1988. In vitro mutagenesis identifies a region within the envelope gene of the human immunodeficiency virus that is critical for infectivity. *Journal of Virology* 62, (1) (Jan): 139-47.

Woodward, C. L., S. Prakobwanakit, S. Mosessian, and S. A. Chow. 2009. Integrase interacts with nucleoporin NUP153 to mediate the nuclear import of human immunodeficiency virus type 1. *Journal of Virology* 83, (13) (Jul): 6522-33.

Yamashita, M., and M. Emerman. 2005. The cell cycle independence of HIV infections is not determined by known karyophilic viral elements. *PLoS Pathogens* 1, (3) (Nov): e18.

Yamashita, M., O. Perez, T. J. Hope, and M. Emerman. 2007. Evidence for direct involvement of the capsid protein in HIV infection of nondividing cells. *PLoS Pathogens* 3, (10) (Oct 26): 1502-10.